

Award Number: W81XWH-05-1-0469

TITLE: Novel Molecular Interactions and Biological Functions of the Neurofibromatosis 2 Tumor Suppressor Protein, Merlin

PRINCIPAL INVESTIGATOR: Olli Carpen, M.D., Ph.D.

CONTRACTING ORGANIZATION: University of Helsinki  
Helsinki 00014 Finland

REPORT DATE: August 2006

TYPE OF REPORT: Annual

PREPARED FOR: U.S. Army Medical Research and Materiel Command  
Fort Detrick, Maryland 21702-5012

DISTRIBUTION STATEMENT: Approved for Public Release;  
Distribution Unlimited

The views, opinions and/or findings contained in this report are those of the author(s) and should not be construed as an official Department of the Army position, policy or decision unless so designated by other documentation.

# REPORT DOCUMENTATION PAGE

*Form Approved*  
*OMB No. 0704-0188*

Public reporting burden for this collection of information is estimated to average 1 hour per response, including the time for reviewing instructions, searching existing data sources, gathering and maintaining the data needed, and completing and reviewing this collection of information. Send comments regarding this burden estimate or any other aspect of this collection of information, including suggestions for reducing this burden to Department of Defense, Washington Headquarters Services, Directorate for Information Operations and Reports (0704-0188), 1215 Jefferson Davis Highway, Suite 1204, Arlington, VA 22202-4302. Respondents should be aware that notwithstanding any other provision of law, no person shall be subject to any penalty for failing to comply with a collection of information if it does not display a currently valid OMB control number. **PLEASE DO NOT RETURN YOUR FORM TO THE ABOVE ADDRESS.**

<b>1. REPORT DATE (DD-MM-YYYY)</b> 01-08-2006			<b>2. REPORT TYPE</b> Annual		<b>3. DATES COVERED (From - To)</b> 29 Jul 2005 – 28 Jul 2006	
<b>4. TITLE AND SUBTITLE</b>  Novel Molecular Interactions and Biological Functions of the Neurofibromatosis 2 Tumor Suppressor Protein, Merlin					<b>5a. CONTRACT NUMBER</b>	
					<b>5b. GRANT NUMBER</b> W81XWH-05-1-0469	
					<b>5c. PROGRAM ELEMENT NUMBER</b>	
<b>6. AUTHOR(S)</b>  Olli Carpen, M.D., Ph.D.  E-Mail: <a href="mailto:olli.carpen@helsinki.fi">olli.carpen@helsinki.fi</a>					<b>5d. PROJECT NUMBER</b>	
					<b>5e. TASK NUMBER</b>	
					<b>5f. WORK UNIT NUMBER</b>	
<b>7. PERFORMING ORGANIZATION NAME(S) AND ADDRESS(ES)</b>  University of Helsinki Helsinki 00014 Finland					<b>8. PERFORMING ORGANIZATION REPORT NUMBER</b>	
<b>9. SPONSORING / MONITORING AGENCY NAME(S) AND ADDRESS(ES)</b> U.S. Army Medical Research and Materiel Command Fort Detrick, Maryland 21702-5012						
<b>10. SPONSOR/MONITOR'S ACRONYM(S)</b>					<b>11. SPONSOR/MONITOR'S REPORT NUMBER(S)</b>	
<b>13. SUPPLEMENTARY NOTES</b>						
<b>14. ABSTRACT</b>  The project studies molecular functions of neurofibromatosis 2 tumor suppressor protein merlin and compares the role of phosphorylation in regulation of merlin and structurally related ezrin. The role of different importin subunits in nuclear targeting of merlin was tested. Merlin bound several importin subunits in a non-selective manner. Merlin was shown to bind tubulin via two different regions, one located in the FERM-domain and one at the C-terminus. Intramolecular association and phosphorylation of S518 residue regulated tubulin binding. Merlin promoted microtubule polymerization in vitro and in vivo. Loss of merlin caused marked changes in microtubule organization and dynamics. Studies on merlin and HEI10, a cell cycle regulator, clarified the interaction mechanism and showed a role for merlin in regulation of the integrity of HEI10. Phosphorylation studies identified a second protein kinase A binding site in merlin. Finally, studies assessing the role of Src-induced tyrosine phosphorylation of ezrin were initiated.						
<b>15. SUBJECT TERMS</b> Neurofibromatosis 2, merlin, ezrin, phosphorylation, PKA, Src, microtubule, cytoskeleton						
<b>16. SECURITY CLASSIFICATION OF:</b>				<b>17. LIMITATION OF ABSTRACT</b>	<b>18. NUMBER OF PAGES</b>	<b>19a. NAME OF RESPONSIBLE PERSON</b> USAMRMC
<b>a. REPORT</b> U	<b>b. ABSTRACT</b> U	<b>c. THIS PAGE</b> U	<b>19b. TELEPHONE NUMBER (include area code)</b>			

## Table of Contents

<b>Introduction.....</b>	<b>4</b>
<b>Body.....</b>	<b>4</b>
<b>Key Research Accomplishments.....</b>	<b>8</b>
<b>Reportable Outcomes.....</b>	<b>9</b>
<b>Conclusions.....</b>	<b>10</b>
<b>References.....</b>	<b>10</b>
<b>Appendices.....</b>	<b>12</b>

## **Introduction**

The neurofibromatosis 2 (NF2) gene product merlin and the ezrin-radixin-moesin (ERM) family protein ezrin are structurally related proteins that demonstrate some functional similarities and interact with each other, but possess opposite effects on cell growth. The experiments of this proposal aim to explore the poorly understood molecular and cell biological basis of the tumor suppressor function of merlin. Specific emphasis has been given to cell cycle stage-dependent targeting of merlin (task 1), analysis of molecular interactions of merlin previously identified by us (tasks 2 and 3), and comparative analysis of phosphorylation-dependent regulation of ezrin and merlin (task 4). All four tasks proposed in the research plan have been pursued and the goals in most tasks have been accomplished. Results from this project and from other groups have opened some new avenues that will be followed. The project was originally recommended to the list of alternate funding on Sept. 24th, 2004. Funding was granted on May 10th, 2005 and the funding period started July 29th, 2005. Due to the over 1 year period between submission of the grant proposal and the initiation of the funding, some progress in the project (especially tasks 3 and 4) was made prior to initiation of the award. This progress will be shortly described below, but these results are not to be included in Reportable Outcomes.

## **Body**

The progress of the project is described in accordance with the tasks outlined in the proposal.

*Task 1. To analyze the mechanisms, regulation and functional consequences of the cell cycle dependent nucleocytoplasmic regulation of merlin.*

To identify factors that regulate nucleocytoplasmic shuttling of merlin, two potential nuclear localization signals (NLS) in merlin (aa 15-20 and aa 309-312) were mutated. These regions consist of a stretch of basic amino acids, which often are involved in nuclear targeting. However, mutation of neither potential NLS affected merlin's transfer into the nucleus. As full-length merlin does not enter nucleus efficiently, similar deletions were introduced into a shorter 4.1-ezrin-radixin-moesin (FERM)-domain construct, merlin 1-339. This construct, when transfected to mammalian cells, can be detected mostly in the nucleus. Again, introduction of the mutations did not prevent nuclear targeting of merlin.

The role of importins in nuclear targeting was tested. We analyzed, whether merlin preferentially binds to certain importin subunits. Recombinant GST-importins were produced, purified and used for pull-down assays (Fig. 1). None of the tested importins were able to bind *in vitro* translated merlin with high affinity. Therefore, we have not pursued this research avenue further.

To study, whether phosphorylation regulates nuclear targeting of merlin, mutants replacing S518 with alanine (A) or aspartate (D) were generated. S518 is a target residue for protein kinase A (PKA) (Alfthan et al. 2004) and p21 activated kinase (PAK) (Kissil et al. 2002). S518A mutant cannot be phosphorylated, whereas S518D is thought to mimic a constitutively phosphorylated protein. Mutant merlin constructs were transfected to cells and compared with wild-type merlin. No differences were detected suggesting that phosphorylation of S518 does not play a role in the regulation of nucleocytoplasmic shuttling. On the other hand, the mutants appear to function in other experiments not related to merlin's nuclear function (see below).

***Task 2.*** *To characterize the association between merlin and microtubules and its functional relevance.*

Both subtasks (a = Identification of tubulin binding sites in merlin and regulation of the interaction) and (b = Functional importance of the interaction between merlin and microtubules) have been carried out and a report of these studies has been submitted for publication (Muranen et al. submitted, see appendix). Two tubulin-binding sites were identified in merlin, one residing at the N-terminal FERM-domain and another at the C-terminal domain (Muranen et al., Fig. 2). The association is transient and can be regulated by merlin's intramolecular association and by phosphorylation of serine 518 (Muranen et al., Fig. 3). Mutant merlin resembling known patient mutations (<http://neurosurgery.mgh.harvard.edu/NFclinic/NFresearch.htm>) showed weakened binding to microtubules (Muranen et al., Fig. 2). Analysis of cultured cells indicated that colocalization between merlin and microtubules depends on cell cycle stage; in synchronized cells merlin and tubulin colocalize only during mitosis at the mitotic spindles and during cytokinesis at the midbody (Muranen et al., Fig. 1). Further analyses on the consequences of merlin deficiency on microtubules were carried out in the most relevant cell type of NF2 disease, *i.e.* the Schwann cell. In primary mouse Schwann cells the two proteins colocalized at the cell membrane (Muranen et al., Fig. 5). In cultured Schwann cells, loss of merlin induced by genetical engineering, caused drastic changes in microtubule organization (Muranen et al., Fig. 5). In further mechanistic studies merlin was demonstrated to promote tubulin polymerization

both *in vitro* and *in vivo* in Schwann cells (Muranen et al., Fig. 6). These results indicate that merlin plays a key role in the regulation of Schwann cell microtubule cytoskeleton and suggest a mechanism by which loss of merlin leads to cytoskeletal defects observed in human schwannomas.

In additional studies, transfected merlin constructs (wild-type WT and merlin 1-547 patient mutant) were transfected to 293HEK and HeLa cells and their effect on spindle formation was evaluated. The results indicated that expression of merlin 1-547 does not colocalize with microtubules in dividing cells and that expression of merlin 1-547 results in an increased amount of multipolar mitotic spindles (Fig. 2). Tubulin was also studied in human mesothelioma cell lines, either expressing or lacking merlin (Pylkkänen et al. 2002) (Fig. 3 and 4). In these cells, a negative correlation was seen between the presence of acetylated tubulin and expression of merlin, whereas a positive correlation was seen between overall tubulin amount and merlin expression, as verified by immunoblotting.

**Task 3.** *To study the role of merlin -- HEI10 interaction and its role in regulation of cell growth.*

A report describing the interaction between merlin and Human Enhancer of Invasion 10 (HEI10) has been published (Grönholm et al. 2006, see appendix). Unfortunately, due to a mistake by the authors, this publication fails to cite the current research contract W81XWH05-1-0469. In this paper, the interaction was shown to be mediated by the  $\alpha$ -helical domain in merlin and the coiled-coil domain in HEI10 and it was shown to require conformational opening of merlin (Grönholm et al., Fig. 1-3). The association appears to be transient *in vivo*, as the two proteins show only partial subcellular colocalization, which depends on cell cycle stage and cell adhesion (Grönholm et al., Fig. 4-5). To study the interplay of the proteins in a relevant cell model, human primary Schwann cell and schwannoma cultures were utilized. Analysis of these cells demonstrated that the distribution of HEI10 depends on merlin expression (Grönholm et al., Fig. 6). Finally, experiments in a cellular transfection model showed that a constitutively open merlin construct affects HEI10 protein integrity (Grönholm et al., Fig. 7). These results link merlin to the cell cycle control machinery and may thus help understanding of its tumor suppressor function.

Further work in these studies has involved generation of HEI10 antibodies. This has proven out to be difficult as recombinant HEI10 is difficult to produce in sufficient quantities and synthetic

HEI10 peptides have been poorly immunogenic. Several attempts to generate novel mouse mAb:s or rabbit antisera have failed. Finally, antisera against HEI10 were raised commercially (AgriSera, Vännäs, Sweden) in chicken using recombinant HEI10 produced by us. Although these antisera recognized HEI10 in ELISA and showed some reactivity against recombinant GST-HEI10 fusion protein, they do not react with transfected or endogenous HEI10 in cellular lysates (Fig. 5). Neither do they recognize HEI10 in immunofluorescence staining. Due to several attempts with negative results, we are not planning to pursue HEI10 antibody production.

**Task 4.** To understand how kinase activity differentially regulates the functional activity of merlin and ezrin.

(a and b). Our previous studies had indicated that the FERM-domain of merlin contains a PKA phosphorylation site (Alfthan et al. 2004). Further experiments using FERM-domain deletion constructs mapped the phosphorylated residue within amino acids 1-100. To identify the amino acid(s) phosphorylated by PKA, *in vitro* mutagenesis of individual potential residues within sequence 1-100 (S10, T24, T58) was carried out. With this method it was demonstrated that residue S10 serves as the only FERM-domain substrate of PKA *in vitro* (Fig. 6). Current efforts aim at generating antibodies that would specifically recognize phosphorylated S10 residue in the FERM-domain. A synthetic phosphopeptide is used as an antigen. Furthermore, mammalian expression constructs, in which S10 has been substituted with alanine (mimics constitutively non-phosphorylated form) or glutamate (mimics constitutively phosphorylated form) have been generated. These will be used in functional studies aiming at understanding the role of S10 phosphorylation *in vivo*.

(c) Most of the goals of Task 4c (Characterization of the Src induced tyrosine phosphorylation of ezrin) were carried out, while the funding was not finalized (alternate funding status) and a report of this work has been published (Heiska and Carpen, 2005). Therefore, the results are only briefly summarized here and not included in Reportable Outcomes. To characterize the Src induced tyrosine phosphorylation of ezrin C-terminus, the potential tyrosines were mutated and phosphorylation of the mutated peptides was analyzed *in vitro*. Residue Y477 was shown to be a major substrate of Src, whereas other residues appeared not to serve as significant substrates (Heiska and Carpen, Fig. 3). The result was confirmed *in vivo* by expressing wild type and mutant ezrin in cells, in which Src family kinase activity can be stimulated (Heiska and Carpen, Fig. 4). A phosphospecific antibody, which recognizes the phosphorylated ezrin Y477 residue

was generated. The antibody works in immunoblotting and further confirms that Y477 is a Src substrate *in vivo* (Heiska and Carpen, Fig. 5). To study phosphorylation-dependent molecular interactions of ezrin, a modified yeast two-hybrid system was utilized. In this approach Src activity can be induced in yeast cells, in which the interaction analysis is carried out. With this technique, a phosphorylation-dependent interaction was identified between ezrin and KTBDDB2, a novel member of Kelch-protein family (Heiska and Carpen, Fig. 8). The interaction was further verified by affinity precipitations, in which Src-phosphorylated GST-ezrin C-terminus and unphosphorylated control is used as a matrix (Heiska and Carpen, Fig. 8).

To further analyze the role of Src induced phosphorylation of ezrin Y477, we have generated stable cell lines with various forms of ezrin with or without Src, using mouse embryonic fibroblasts (MEF) from ezrin knock-out mice (Saotome et al. 2004) as parent cells. For establishing the stable ezrin add-back lines, the wild-type and the mutant versions of the full-length ezrin cDNA were introduced to pBABEpuro vector (Morgenstern et., 1990). 293 Eco Phoenix retrovirus packaging cell line was transfected with the different constructs, the virus containing supernatant collected and used in the transduction of the MEFs. The expression vector containing cell populations were selected with 2.5 mg/ml of puromycin in the medium. To express constitutively active Src, the cells were further introduced with a retroviral construct pLXSH-SrcY527F (Cary et al 2002), provided by Dr. J. A. Cooper (Fred Hutchinson Cancer Research Center, Seattle, WA), and selected with 0.25 mg/ml of hygromycin B (Fig. 7). The cells will be used to evaluate the neoplastic features induced by Src, and the ability of merlin to suppress the potential oncogenic phenotype.

## Key Research Accomplishments

- Identification of two tubulin binding sites in merlin
- Demonstration that the interaction with tubulin is regulated by intramolecular association and phosphorylation of merlin
- Demonstration that merlin regulates microtubule polymerization *in vitro* and *in vivo*
- Demonstration that microtubule cytoskeleton is markedly altered in Schwann cells lacking merlin
- Detailed molecular characterization of the interaction between merlin and HEI10
- Demonstration that merlin regulates the integrity of HEI10 *in vivo*
- Identification of a second protein kinase A substrate residue in merlin



## **Reportable Outcomes**

### *Publications:*

Grönholm M., T. Muranen, G. Toby, T. Utermark, CO. Hanemann, EA. Golemis, O. Carpén. A functional association between merlin and HEI10, a cell cycle regulator. *Oncogene* 25:4389-4398, 2006. (Due to authors' error, this publication does not cite the current research contract W81XWH05-1-0469).

Muranen, T., M. Grönholm, A. Lampin, D. Lallemand, F. Zhao, M. Giovannini, O. Carpén. The tumor suppressor merlin interacts with microtubules and modulates Schwann cell microtubule cytoskeleton. Submitted.

Grönholm M. Novel Functions of the Neurofibromatosis 2 Tumour Suppressor Protein Merlin. Ph.D. Thesis, Faculty of Medicine, University of Helsinki, Finland. 2005. (Award for best thesis of the Faculty of Medicine, University of Helsinki, in 2005)

Laulajainen M. Characterization of merlin's cell-extension activity. M. Sc. Thesis. Department of Biological and Environmental Sciences, University of Helsinki, Finland. 2005.

### *Presentations:*

4-6.6. 2006. Minja Laulajainen, Carboxy-terminus regulates morphogenic activities of merlin. Poster presentation. 2006 Children's Tumor Foundation International Neurofibromatosis Consortium. Aspen, CO.

4-6.6. 2006. Taru Muranen, Merlin interacts with microtubules in a regulated manner and affects the microtubule cytoskeleton of the mouse primary Schwann cells. Poster presentation. 2006 Children's Tumor Foundation International Neurofibromatosis Consortium. Aspen, CO.

### *Degrees:*

Grönholm M. Ph. D. degree, University of Helsinki, Finland 2005.

Laulajainen M. M. Sc. University of Helsinki, Finland, 2005.

### *Novel research tools:*

retroviral plasmid constructs of wild-type ezrin and ezrin Y477F, ezrin Y145F and ezrin Y353F mutants for expression in mammalian cells

stable MEF cell lines expressing wild-type or mutant (Y145F, Y353F, Y477F) cell lines with or without constitutively active Src.

plasmid constructs with altered merlin S10 and S518 residues

## Conclusions

The research project has advanced well in all areas related to the four main tasks. The work has resulted in several interesting observations on the biology of the NF2 tumor suppressor protein, merlin, and in one publication and one submitted manuscript. We have identified a novel function for merlin as a regulator of microtubule cytoskeleton. This is a timely finding as independent studies have indicated a role for merlin in growth factor receptor endocytosis, an event controlled by microtubules (Maitra et al. 2006). Studies between merlin and HEI10 have provided findings that for the first time link merlin directly to molecules involved in cell cycle regulation.

Posttranslational modification via phosphorylation seems to be an important mechanism in the regulation of both merlin and ezrin. An additional demonstration of this was recent identification of a merlin phosphatase and demonstration that inhibition of the phosphatase prevents merlin's tumor suppressor activity (Jin et al. 2006). Our studies focus on kinase activity, the other side of the coin. The results extend previous findings on the interplay between PKA signaling pathway and merlin by identifying a second PKA phosphorylation site in merlin. PKA activity has been linked to increased proliferative potential of Schwann cells (Kim et al. 1997). As Schwann cells are susceptible to tumor formation in NF2 disease, our findings may provide clues on the molecular pathways involved in this tumorigenic events. Finally, the association between Src family kinases and ezrin may prove out to be of importance for understanding of NF2 disease. Src activity is associated with proliferative activity of Schwann cells, and thus the findings may have relevance in the biology of schwannomas, the hallmark tumors of NF2.

## References

Alfthan K., Heiska L., Grönholm M., Renkema G.H. and Carpen O. (2004) Cyclic AMP-dependent protein kinase phosphorylates merlin at serine 518 independently of P21-activated kinase and promotes merlin-ezrin heterodimerization. *J. Biol. Chem.*, **279**, 18559-18566.

Cary LA, Klinghoffer RA, Sachsenmaier C, Cooper JA. (2002) SRC catalytic but not scaffolding function is needed for integrin-regulated tyrosine phosphorylation, cell migration, and cell spreading. *Mol Cell Biol.* **8**, 2427-2440.

Heiska, L., O. Carpén. Src phosphorylates ezrin at tyrosine 477 and induces a phosphospecific interaction between ezrin and a kelch-repeat protein family member. (2005) *J. Biol. Chem.* **280**, 10244-10252.

Jin H., Sperka T., Herrlich P. and Morrison H. (2006) Tumorigenic transformation by CPI-17 through inhibition of a merlin phosphatase. *Nature*, **442**, 576-579.

Kissil J.L., Johnson K.C., Eckman M.S. and Jacks T. (2002) Merlin phosphorylation by p21-activated kinase 2 and effects of phosphorylation on merlin localization. *J. Biol. Chem.*, **277**, 10394-10399.

Maitra S., Kulikauskas R.M., Gavilan H. and Fehon R.G. (2006) The tumor suppressors merlin and expanded function cooperatively to modulate receptor endocytosis and signaling. *Curr. Biol.*, **16**, 702-709.

Morgenstern JP, Land H. (1990) Advanced mammalian gene transfer: high titre retroviral vectors with multiple drug selection markers and a complementary helper-free packaging cell line. *Nucleic Acids Res.* **18**, 3587-3596.

Pylkkänen L., Sainio M., Ollikainen T., Mattson K., Nordling S., Carpen O., Linnainmaa K., Husgafvel-Pursiainen K. (2002) Concurrent LOH at multiple loci in human malignant mesothelioma with preferential loss of NF2 gene region *Oncol. Rep.*, **9**, 955-959.

Saotome I, Curto M, McClatchey AI. (2004) Ezrin is essential for epithelial organization and villus morphogenesis in the developing intestine. *Dev. Cell.* **6**, 855-864.

## Appendices

### *Figure legends:*

**Figure 1. Interaction between merlin and importins.** Recombinant GST-importin  $\alpha$  and  $\beta$ -subunits were produced in insect cells, purified and bound to glutathione-Sepharose beads.  $^{35}\text{S}$ -methionine labeled full-length merlin was produced by *in vitro* translation (IVT) in rabbit reticulocyte lysates. IVT-merlin was pulled down with GST-importins and precipitates were run on SDS-PAGE. IVT produced nucleoprotein was used as a positive control with GST-importin  $\alpha$ -5 and plain GST as a negative control. Merlin does not show preferential binding to any of the importin subunits.

**Figure 2. Merlin 1-547 does not colocalize with tubulin and alters the morphology of mitotic structures.** **a**, 293 cells stably expressing wild-type (wt) merlin or a carboxy-terminal deletion construct (1-547) were double-stained for merlin and tubulin. Wild-type merlin and tubulin colocalize in mitotic spindles in analogy with endogenous merlin. In contrast, merlin 1-547 accumulates underneath the cortical membrane without any colocalization with tubulin. **b-c**, 293HEK cells transfected with wt merlin or merlin 1-547 were evaluated for the morphology of mitotic figures. The figures were categorized as unipolar, normal or multipolar and their number was counted. Mean percentage  $\pm$  SE from four different experiments is shown. Mitotic figures of cells overexpressing wild-type merlin do not differ from control cells, whereas cells expressing merlin 1-547 have a significantly higher number of multipolar spindles. Scale bar 30  $\mu\text{m}$ .

**Figure 3. Lack of merlin correlates with the presence of acetylated tubulin in human malignant mesothelioma cell lines.** Five patient mesothelioma cell lines were blotted for merlin and acetylated tubulin. Mesothelioma cell lines M14 and M38 expressed merlin whereas lines M10, M25 and M146 did not. The expression of acetylated tubulin correlated negatively with and the presence of tubulin correlated positively with merlin expression. Ezrin was used as a loading control. Acetylated tubulin marks the presence of older and more rigid microtubular structures.

**Figure 4. Immunocytochemical analysis of acetylated tubulin in mesothelioma cell lines.** Mesothelioma cells were immunostained for acetylated tubulin. In line with immunoblotting result acetylated tubulin staining was more intensive in cells lacking merlin (cell lines M10K, M25K, M146K) as compared to those expressing merlin (M14K, M38K).

**Figure 5. Analysis of HEI10 antibody produced in chicken.** Polyclonal IgY antibody was produced by immunizing chicken with recombinant aGST-HEI10 fusion protein. Preliminary screening by ELISA indicated that the antiserum recognizes recombinant GST-HEI10. For further testing 293 HEK cells were transfected HA-tagged HEI10, the cells were lysed, lysates run on SDS-PAGE and immunoblotted with chicken antiserum or with HA-antibody. The chicken HEI10 antibody (right) does not recognize the transfected HEI10, which is detected by anti-HA antibody (left).

**Figure 6. Identification of S10 as a protein kinase A target residue in merlin.** Bacterially expressed GST-merlin fusion proteins were phosphorylated *in vitro* using  $\{\gamma\text{-}^{33}\text{P}\}$ ATP and purified catalytic subunit of PKA. Proteins were separated on SDS-PAGE. A, Mapping of the phosphorylation site. Potential phosphorylation sites were mutated to alanine in a construct containing merlin residues 1-100. Left panel shows Coomassie blue staining and right panel is an autoradiograph. Arrows depict merlin. Merlin 1-100 is phosphorylated whereas control GST is not. Mutation of S10A completely abolishes phosphorylation, whereas other mutations do not have an effect. B, N-terminal FERM-domain (1-314) of merlin with and without serine 10 mutation or GST-fusion protein were phosphorylated with PKA and analyzed as above. The mutation had the same effect in merlin 1-314 (shown by arrowhead) as in merlin 1-100 indicating that serine 10 is the only N-terminal residue phosphorylated by PKA *in vitro*.

**Figure 7. Characterization of the ezrin -/- MEF cells and their addback subclones.** A. Cell lysates were separated by SDS-PAGE and immunoblotted with a polyclonal anti-ezrin antibody. WT = ezrin wild-type; ctr = vector control (pBABEpuro); Y145F = ezrin Y145F mutant; Y477F = ezrin Y477F mutant; Src CA = constitutively active Src. B. The same cell lysates were probed with an anti-moesin antibody. C. The lysates were probed with an antibody recognizing phosphorylated T588moesin. D. The lysates were probed with an antibody recognizing active Src (phosphorylated on Y418). E. Ezrin was immunoprecipitated from cell lysates and tyrosine phosphorylation was detected with an anti-phosphotyrosine antibody (left panel). The same filter was stripped and subsequently probed with the anti-ezrin antibody (right panel). WCL = whole

cell lysate; pre-imm = preimmune control immunoprecipitation. The arrows indicate the positions for the specific bands in each subfigure.

Figures 1-7.

#### Articles and manuscript

Grönholm M., T. Muranen, G. Toby, T. Utermark, CO. Hanemann, EA. Golemis, O. Carpen. A functional association between merlin and HEI10, a cell cycle regulator. (2006) *Oncogene* **25**:4389-4398.

Muranen, T., M. Grönholm, A. Lampin, D. Lallemand, F. Zhao, M. Giovannini, O. Carpen. The tumor suppressor merlin interacts with microtubules in a regulated manner and modulates the microtubule cytoskeleton of Schwann cells. Submitted for publication.

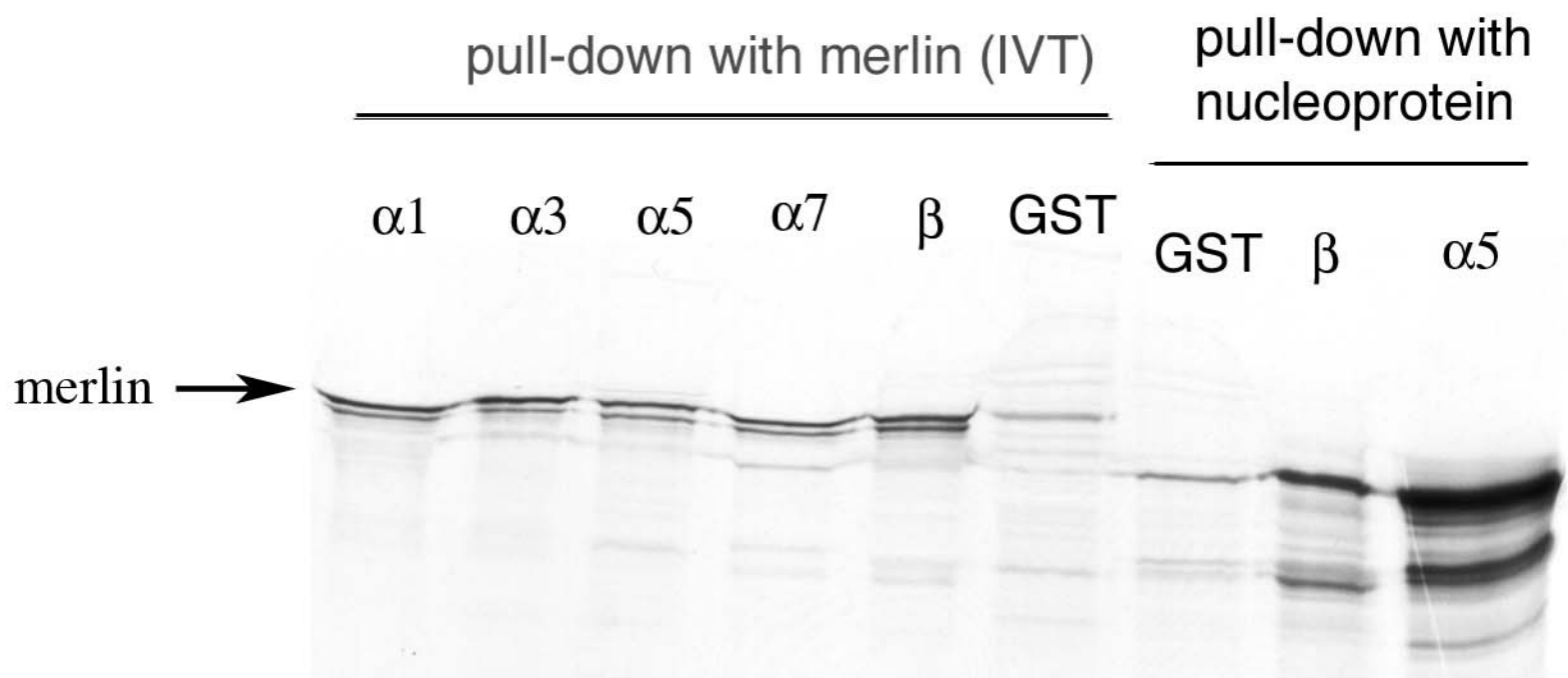


Figure 1

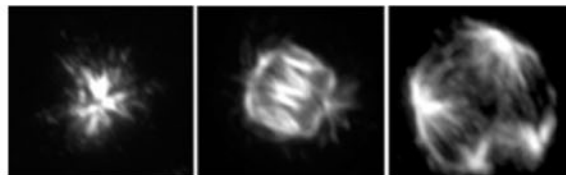
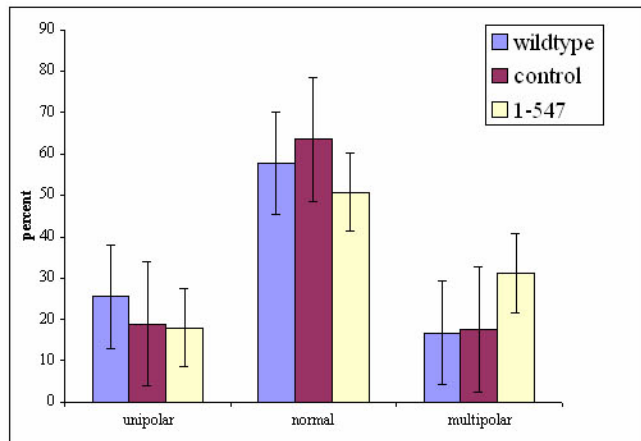
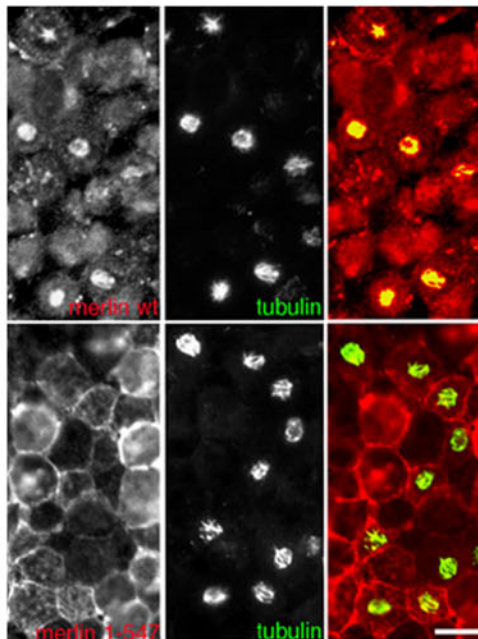


Fig. 2



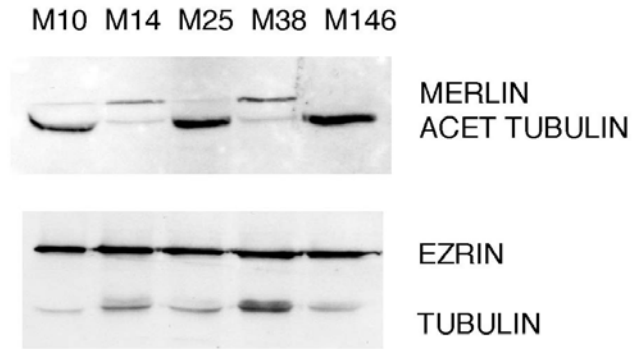


Figure 3

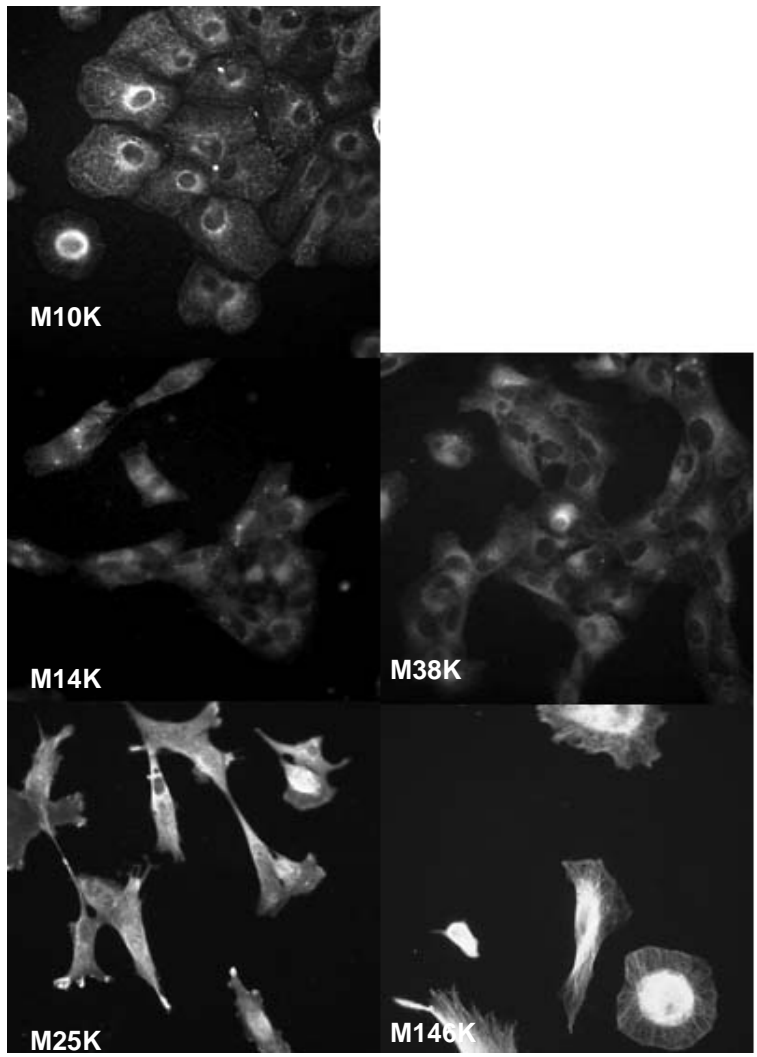


Figure 4

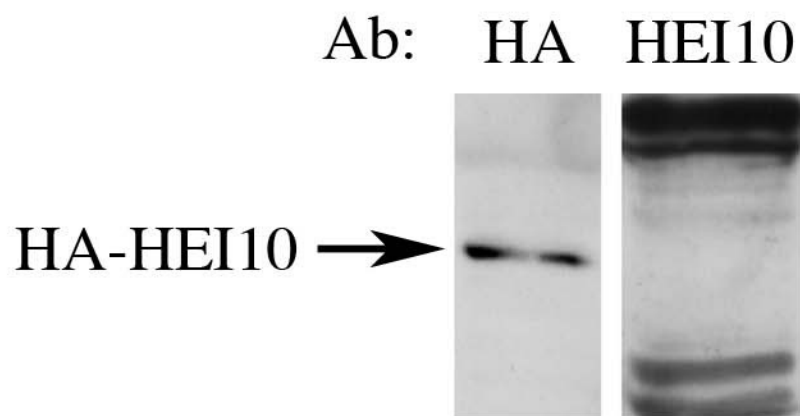
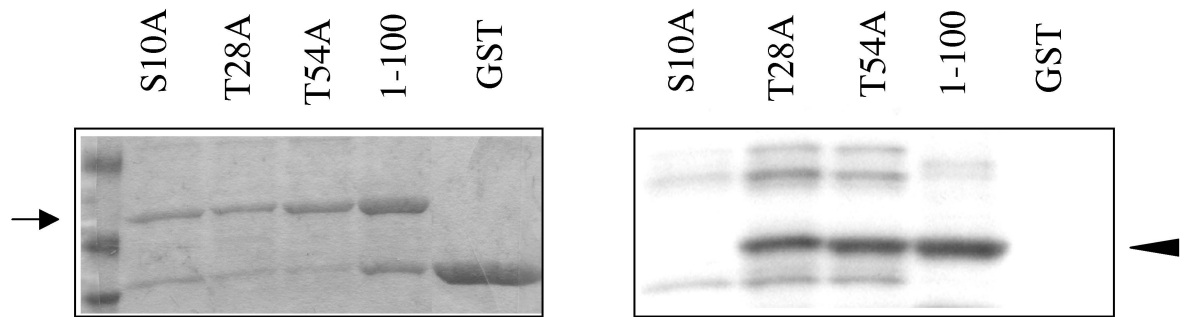


Figure 5

A.



B.

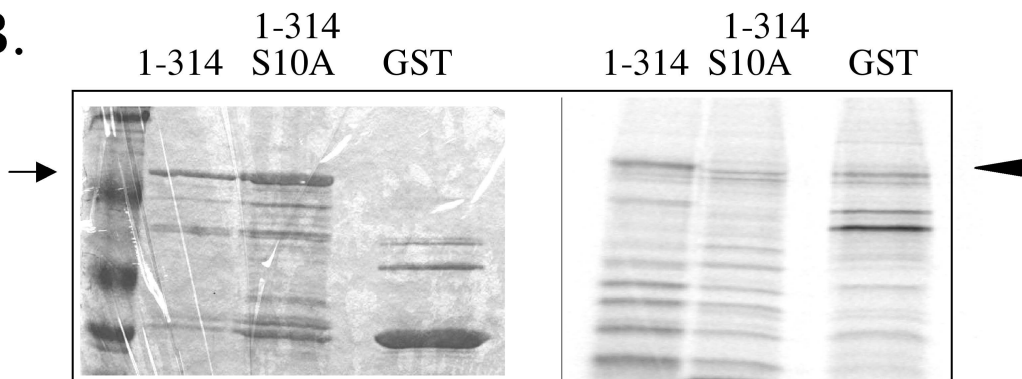


Figure 6

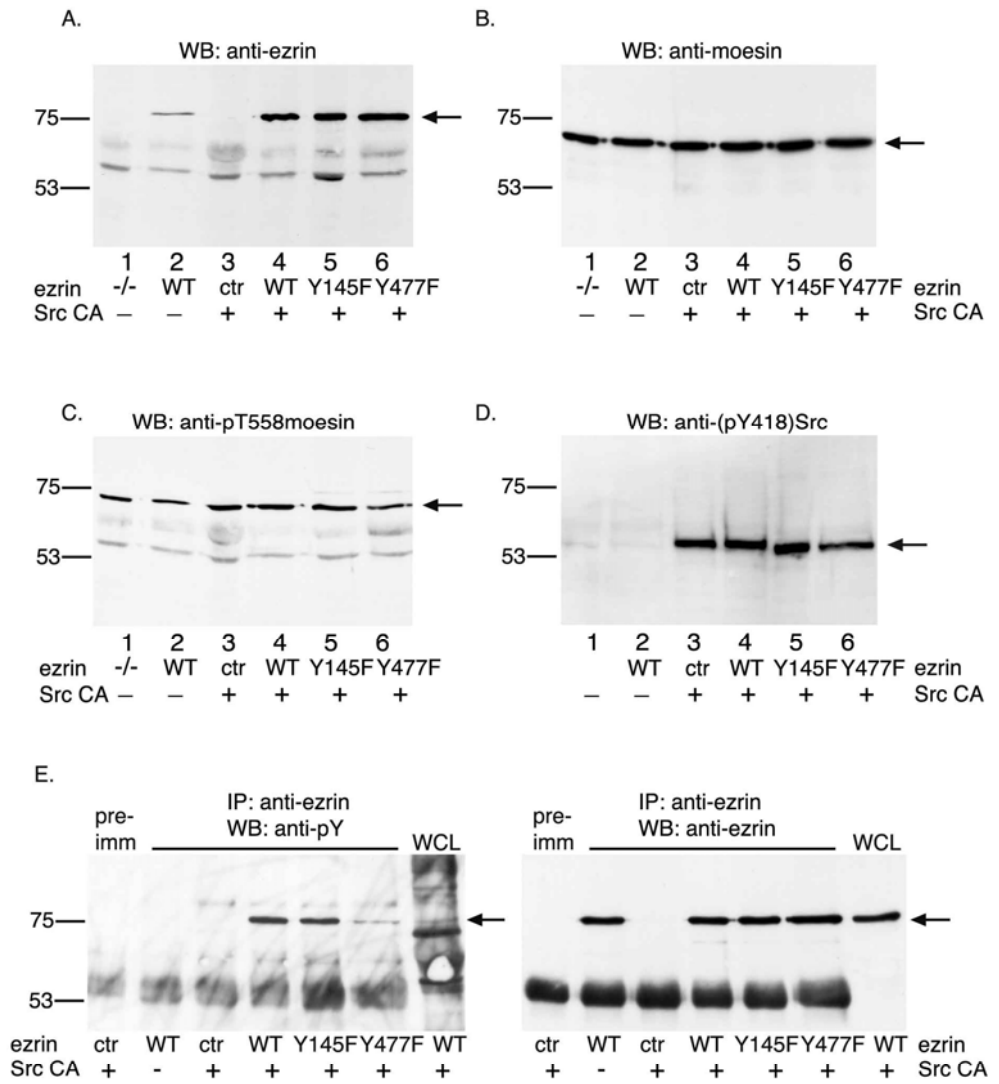


Figure 7

## ORIGINAL ARTICLE

**A functional association between merlin and HEI10, a cell cycle regulator**M Grönholm<sup>1,6</sup>, T Muranen<sup>1,6</sup>, GG Toby<sup>2</sup>, T Utermark<sup>3</sup>, CO Hanemann<sup>4</sup>, EA Golemis<sup>2</sup> and O Carpén<sup>1,5</sup><sup>1</sup>Neuroscience Program, Biomedicum Helsinki, Department of Pathology, University of Helsinki and Helsinki University Central Hospital, Helsinki, Finland; <sup>2</sup>Division of Basic Science, Fox Chase Cancer Center, Philadelphia, PA, USA; <sup>3</sup>Department of Neurology, University of Ulm, Ulm, Germany; <sup>4</sup>Clinical Neurobiology, Institute of Clinical and Biomedical Science, Peninsula Medical School, Plymouth, UK and <sup>5</sup>Department of Pathology, University of Turku and Turku University Hospital, Turku, Finland

**Merlin and ezrin are homologous proteins with opposite effects on neoplastic growth. Merlin is a tumor suppressor inactivated in the neurofibromatosis 2 disease, whereas upregulated ezrin expression is associated with increased malignancy. Merlin's tumor suppressor mechanism is not known, although participation in cell cycle regulation has been suggested. To characterize merlin's biological activities, we screened for molecules that would interact with merlin but not ezrin. We identified the cyclin B-binding protein and cell cycle regulator HEI10 as a novel merlin-binding partner. The interaction is mediated by the alpha-helical domain in merlin and the coiled-coil domain in HEI10 and requires conformational opening of merlin. The two proteins show partial subcellular colocalization, which depends on cell cycle stage and cell adhesion. Comparison of Schwann cells and schwannoma cultures demonstrated that the distribution of HEI10 depends on merlin expression. In transfected cells, a constitutively open merlin construct affected HEI10 protein integrity. These results link merlin to the cell cycle control machinery and may help to understand its tumor suppressor function.**

*Oncogene* (2006) **25**, 4389–4398. doi:10.1038/sj.onc.1209475; published online 13 March 2006

**Keywords:** NF2; ERM; HEI10

**Introduction**

Inherited mutations of the neurofibromatosis 2 (*NF2*) gene, which encodes for merlin, result in the development of numerous nervous system tumors; schwannomas, meningiomas and ependymomas, in the dominantly inherited *NF2* disease (Louis *et al.*, 1995). Biallelic *NF2* gene inactivation has also been demonstrated in other tumor types, especially mesotheliomas

(Arakawa *et al.*, 1994; Pineau *et al.*, 2003). The *NF2* tumor suppressor protein merlin (schwannomin) is related to the ezrin–radixin–moesin (ERM) protein family. Ezrin–radixin–moesin proteins are associated with the actin cytoskeleton and cell membrane components and are involved in membrane structure morphogenesis, cell adhesion, membrane traffic, cell signaling and the regulation of cell growth (Bretscher *et al.*, 2002).

Inter- and intramolecular associations regulate merlin's functions and interactions with other proteins (Gonzalez-Agosti *et al.*, 1999; Grönholm *et al.*, 1999). Two types of kinases, PAK-1/2 and PKA have been shown to phosphorylate merlin at serine 518 and regulate its activity (Kissil *et al.*, 2002; Xiao *et al.*, 2002; Alftan *et al.*, 2004), but it is still unclear, whether the phosphorylation is sufficient to release the intramolecular bond between the N-terminal FERM domain and the C-terminus.

In spite of many studies, the tumor suppressor function of merlin is not yet understood. Some evidence indicates that merlin is involved in cell cycle control. Overexpression of merlin can inhibit cell proliferation (Lutchman and Rouleau, 1995; Sherman *et al.*, 1997; Gutmann *et al.*, 1999) and transfection of merlin into primary schwannoma and mesothelioma cells reduces proliferation and promotes G0/G1 arrest (Schulze *et al.*, 2002; Xiao *et al.*, 2005). Conversely, suppression of merlin in tumor cells induces proliferation (Huynh and Pulst, 1996) and a targeted disruption of the *NF2* gene results in increased cell proliferation and tumor formation (McClatchey, 2003). In accordance with a role for merlin in cell cycle regulation, we recently demonstrated cell cycle-dependent nucleo-cytoplasmic shuttling of merlin (Muranen *et al.*, 2005). To get insight into merlin's mechanism of action in cell cycle control we exploited the fact, that in spite of structural homology, overlapping subcellular distribution, direct association and partially overlapping protein interactions, merlin and ezrin exert opposite effects on cell growth. Indeed, increased expression of ezrin is associated with enhanced cell growth and poor prognosis of malignant tumors (Geiger *et al.*, 2000; Mäkitie *et al.*, 2001; Khanna *et al.*, 2004; Tynninen *et al.*, 2004; Ilmonen *et al.*, 2005). To provide clues on how merlin exerts its growth regulatory activity, we therefore sought to identify binding partners which are specific for merlin or ezrin.

Correspondence: Dr M Grönholm, Neuroscience Program, Biomedicum Helsinki, Haartmanink. 8, PB 63, Helsinki 00014, Finland. E-mail: mikaela.gronholm@helsinki.fi

<sup>6</sup>These authors contributed equally to this work.

Received 4 October 2005; revised 16 December 2005; accepted 10 January 2006; published online 13 March 2006

HEI10 is a recently identified cell cycle regulator in both yeast and vertebrate cells (Toby *et al.*, 2003). HEI10 encodes a 277 amino-acid protein, which consists of an N-terminal RING-finger motif characteristic of E3 ubiquitin ligase, a coiled-coil domain and a C-terminal domain with a VSPSR motif, which is phosphorylated by cyclin B/cdc2. The N-terminal part of HEI10 interacts with the UbcH7 E2 ubiquitin conjugating enzyme and both interacts with and controls the accumulation of cyclin B, a key protein in cell cycle control (Toby *et al.*, 2003). The *HEI10* gene is a component of a translocation fusion to the *HMG1C* gene in uterine leiomyoma (Mine *et al.*, 2001) and altered HEI10 expression has been seen in melanomas (Smith *et al.*, 2004). These results imply that the deregulation of HEI10 may have consequences for tumor development. Here, we provide *in vitro* and *in vivo* evidence of a direct interaction between merlin and HEI10 and a role for merlin in regulation of HEI10 expression.

## Results

### Interaction of merlin and HEI10

To identify novel interaction partners specific for merlin but not ezrin we performed a yeast two-hybrid screen of a HeLa cell library using merlin 252–595 as bait. This construct was chosen instead of the full-length protein, since previous studies have shown that N- or C-terminally truncated merlin mimics an open conformation, where binding sites to other proteins are accessible (Grönholm *et al.*, 1999). The screen identified HEI10 as a novel binding partner for merlin. In a mating assay merlin constructs 1–546 and 252–595, but not ezrin constructs 1–309 and 278–585, interacted with HEI10 (Figure 1a). To further study the interaction, *in vitro* binding assays were performed. *In vitro* translation (IVT)-produced merlin 1–595 (wt) or merlin 1–547, which have previously been shown to mimic a constitutively open conformation (Grönholm *et al.*, 1999), was mixed with glutathione-coupled glutathione *S*-transferase (GST)-HEI10 46–277 or GST and bound proteins detected with SDS-PAGE and autoradiography. Glutathione *S*-transferase-HEI10 46–277 but not GST alone pulled down merlin 1–547 and merlin 1–595. In a reciprocal experiment, GST-merlin 1–547 but not GST alone pulled down IVT-produced HEI10 1–277 (wt) (Figure 1b).

In an additional interaction test, HA-tagged merlin and ezrin constructs were produced in yeast and yeast lysates were used for pull down assays with glutathione-bound GST-HEI10 46–277. Glutathione *S*-transferase-HEI10 46–277 pulled down merlin constructs 1–546 and 252–595, both of which contain the alpha-helical part of merlin. Full-length merlin or merlin constructs containing only the N-terminal domain 1–314 or the C-terminal domain 492–595, were not precipitated by GST-HEI10 46–277 (Figure 1c, for domain structure see Figure 3). Again, no association was seen between ezrin and HEI10.

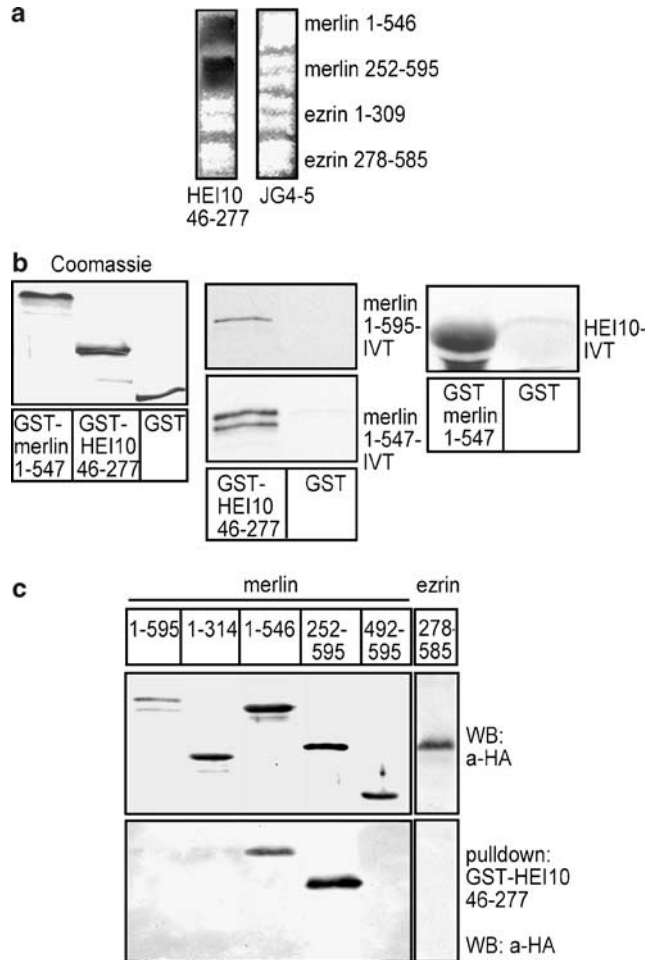


**Figure 1** Interaction studies of merlin and HEI10. (a) A yeast two-hybrid analysis of the interaction between merlin and HEI10. Both merlin baits interact with HEI10 46–277, whereas ezrin baits show no reactivity. The empty vector JG4-5 was used as a control. (b) Interaction between glutathione *S*-transferase (GST)-fusion constructs and *in vitro* translated proteins. Left panel shows Coomassie blue staining of purified GST-tagged merlin 1–547 and HEI10 46–277 constructs. In middle panel, *in vitro* translated merlin 1–595 (wt) or 1–547 were incubated with glutathione agarose-coupled GST-HEI 46–277 or GST alone. Bound protein was detected with autoradiography. Right panel, shows a reciprocal experiment in which *in vitro* translated HEI10 1–277 was allowed to bind GST-merlin 1–547 or GST containing beads. (c) HA-tagged merlin and ezrin constructs were produced in yeast and their expression verified with anti-HA monoclonal antibody (mAb) (left panel). Lysates from yeast expressing HA-tagged merlin and ezrin constructs were incubated with glutathione agarose-coupled GST-HEI10 46–277. Bound proteins were detected using the anti-HA mAb (right panel).

The HEI10 rabbit antiserum is not functional in immunoprecipitations. Therefore, to study whether merlin and HEI10 interact in cells, 293HEK cells stably expressing merlin 1–595 (wt) or merlin 1–547 were transfected with HA-tagged HEI10. Cells were lysed 24 h after transfection and lysates immunoprecipitated with anti-HA monoclonal antibody (mAb). Filters were immunoblotted with merlin antibody or with anti-HA mAb. Merlin 1–547 (Figure 2b), but not merlin wild type (wt) (Figure 2a), could be coprecipitated with HA-HEI10.

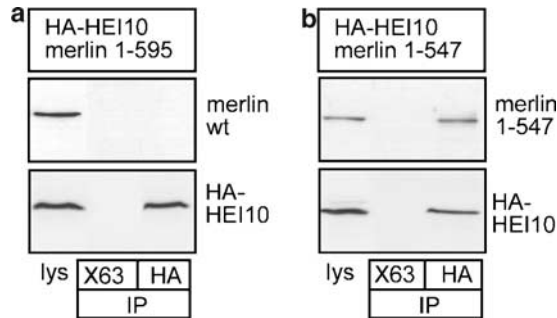


**Figure 2** Coimmunoprecipitation of merlin and HEI10 from 293HEK cells. 293HEK cells stably expressing merlin wild type (wt) (a) or merlin 1–547 (b) were transfected with HA-HEI10. 24 h after transfection cells were lysed (lys) and used for immunoprecipitation with X63 control monoclonal antibody (mAb) or HA mAb. Precipitated proteins were detected with merlin A19 rabbit antiserum or anti-HA mAb.

### Mapping of the merlin and HEI10 interaction sites

The yeast two-hybrid method and various merlin and HEI10 deletion constructs and mutants were used to further map the interaction sites in merlin and HEI10. Only constructs containing the alpha-helical region of merlin interacted with HEI10 (Figure 3a). The region between merlin 306 and 339 contained critical residues, since the alpha-helical sequence 306–478 bound HEI10, but the N-terminal construct 1–314 or C-terminal construct 339–595 did not. A HEI10 construct containing the coiled-coil domain (residues 116–200) was sufficient for the interaction, while neither the N-terminal RING-finger domain nor the C-terminal domain containing the cyclin B/cdc2 phosphorylation site bound merlin. Binding was retained in merlin 252–595 with patient missense mutations L316T or L316W, or an amino-acid substitution (A468P), which completely disrupts the PKA-R1 $\beta$ -binding site (Grönholm *et al.*, 2003).

To further map the interaction site we created a transposon mutation library of merlin 1–546 with randomly introduced 15 bp in-frame insertions, each encoding five extra amino acids. Constructs were tested against HEI10 1–200 binding in the yeast two-hybrid system. Seven independent insertions within amino acids 275–326 disrupted binding of merlin to HEI10. Four of these insertions; at amino acids 306, 307, 318 and 326 localized within the previously mapped critical region, while two (275 and 283) were localized immediately before the interaction domain. One insertion within this region, at amino acid 277, did not affect binding. None of the other insertions prior to amino acid 275 at the end of the FERM-domain or the more C-terminal part of the alpha-helix affected HEI10 binding (Figure 3b).

**Distribution of merlin and HEI10 in osteosarcoma cells**  
We recently demonstrated that the subcellular distribution of merlin is altered during adhesion and cell cycle progression in many cell types including U2OS osteosarcoma cells, which express both merlin (Muranen *et al.*, 2005) and HEI10 (Toby *et al.*, 2003). To evaluate

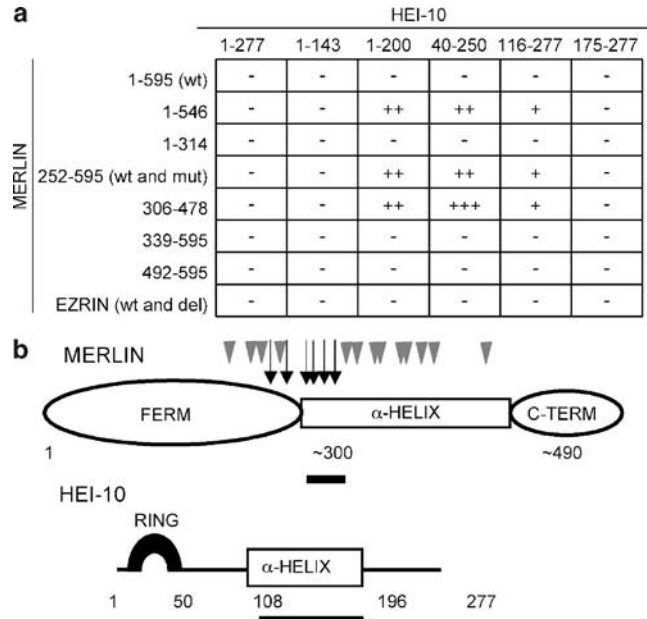


**Figure 3** Interaction analysis of merlin and HEI10 using the yeast two-hybrid system. (a) Merlin bait constructs were tested against HEI10 prey constructs for interactions in a yeast two-hybrid mating assay. Numbers represent amino acids, + - + + + indicate weak to strong color reaction, a marker of an interaction and - indicates lack of interaction. Merlin 252–595 includes the normal construct and one with an introduced PKA-binding site mutation A468P as well as known patient mutations L316W and L316F, which all bound with identical strength. Ezrin represents 1–585 (wt) and deletion constructs (del) 1–309 and 278–585. (b) A mutation library of merlin two-hybrid construct 1–546 with randomly introduced 5 amino-acid insertions was used to test the interaction with HEI10 1–200 in a yeast two-hybrid mating assay. Insertions in positions indicated by black arrows abolished the interaction with HEI10 and grey arrowheads represent insertions that do not alter the interaction. Black bars underneath merlin and HEI10 represent the critical residues required for binding; merlin amino acids 306–339 and HEI10 116–200, based on the constructs used.

whether merlin and HEI10 are targeted in a similar fashion, cells were trypsinized and allowed to reattach. During early reattachment, both merlin and HEI10 were localized to the nucleus (Figure 4a). However, as cells started to spread, merlin and HEI10 could be seen in punctuate structures at the plasma membrane. At this stage, a significant fraction of HEI10 was still present in the nucleus but most of the merlin immunoreactivity had exited the nucleus (Figure 4b). When the cells were more fully spread, merlin and HEI10 could be seen in the submembranous compartment and diffusely in the cytoplasm (Figure 4c).

### The colocalization of merlin and HEI10 in U2OS cells is dependent on cell cycle stage

In order to study the localization of HEI10 at different phases of the cell cycle, subconfluent U2OS cells were synchronized using nocodazole or mimosine treatment. FACS analysis was used to confirm the efficiency of synchronization and to monitor the cell cycle phase after block release (not shown). This experiment revealed that



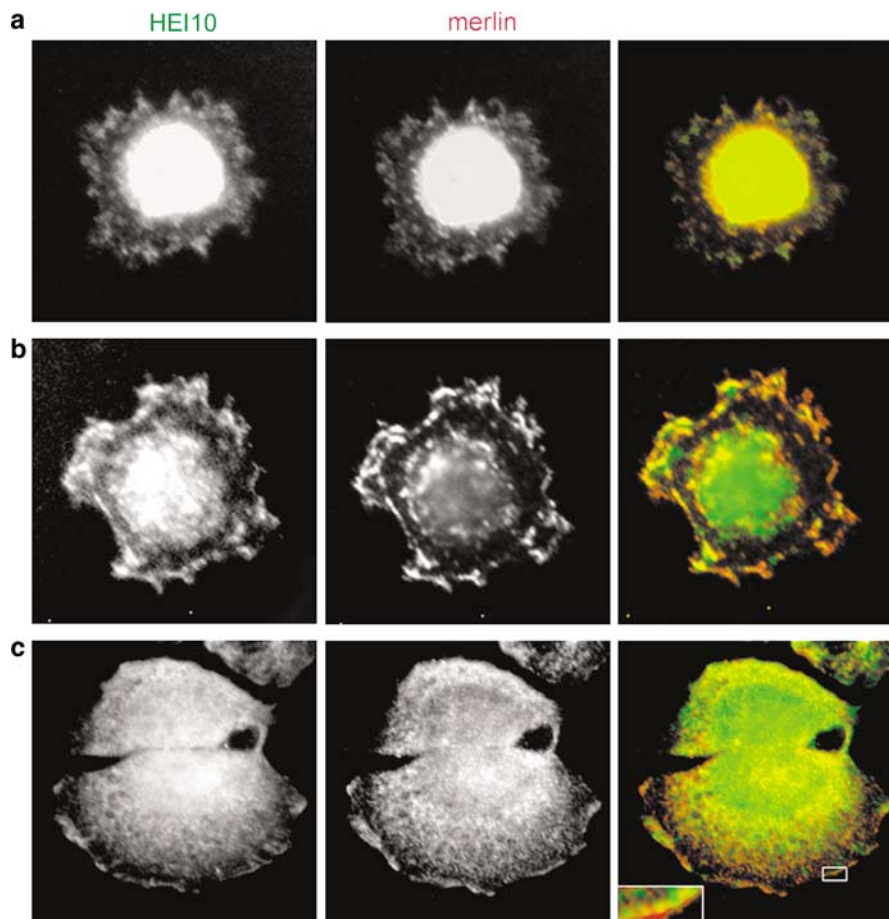


**Figure 4** Localization of merlin and HEI10 in osteosarcoma cells. U2OS cells expressing endogenous merlin and HEI10 were trypsinated and allowed to reattach for 30 min (a), 1 h (b) or 2 h (c). Cells were fixed and stained with merlin IC4 monoclonal antibody (mAb) and HEI10 rabbit antiserum and images taken with an epifluorescence microscope. Both proteins are present primarily in the nucleus as cells are attaching. HEI10 persists in the nucleus longer than merlin during reattachment and spreading. A partial colocalization, particularly at the membrane (inset), can be seen in fully spread cells.

HEI10 localization varied in a cell cycle-specific manner. HEI10 colocalized with merlin in some but not all stages of the cell cycle (Figure 5). In early G1 merlin and HEI10 were present in the nucleus but both proteins rapidly disappeared from the nucleus as cells progressed in G1. HEI10 returned to the nucleus in S-phase, remaining in this compartment until mitosis. In contrast, merlin remained at the cell periphery until late G2, at which state the protein accumulated in the perinuclear region. During the entire cell cycle a fraction of both proteins could also be found at the membrane. We recently showed that merlin is concentrated in the mitotic spindle of dividing cells and to the midbody during cytokinesis (Muranen *et al.*, 2005). In U2OS cells stained for HEI10, tubulin and DNA, also HEI10 associated with microtubules at the mitotic spindle and the contractile ring (Figure 5).

*The localization of HEI10 is dependent on merlin expression level*

To study if the distribution of HEI10 is dependent on the expression level of merlin, we compared the RT4 rat

schwannoma cell line with a merlin-inducible RT4-5-4 variant (Figure 6). RT4 cells express very low amounts of merlin, but expression of merlin can be induced with doxycycline in RT4-5-4 cells. In RT4 cells, HEI10 was seen in nuclei and diffusely in the cytoplasm, while weak merlin reactivity was detected underneath the cell membrane. RT4-5-4 cells with induced merlin expression showed a different HEI10 staining pattern. In some cells merlin and HEI10 colocalized in extensions and at the membrane (Figure 6f). In around 10% of RT4-5-4 cells (an estimation from 500 counted cells) the nucleus was completely devoid of merlin and HEI10 (Figure 6f and f'). Cells, in which merlin expression was not induced demonstrated strong nuclear HEI10 reactivity (Figure 6f and f'').

HEI10 localization was also studied in primary human schwannoma and Schwann cell cultures, which by immunoblotting were verified to express HEI10 (not shown). In schwannoma cells, which do not express merlin due to biallelic *NF2* gene inactivation, HEI10 was frequently localized the nucleus (Figure 6h) in line with rat schwannoma cells. On the other hand, in Schwann cells, which express merlin (not shown) HEI10

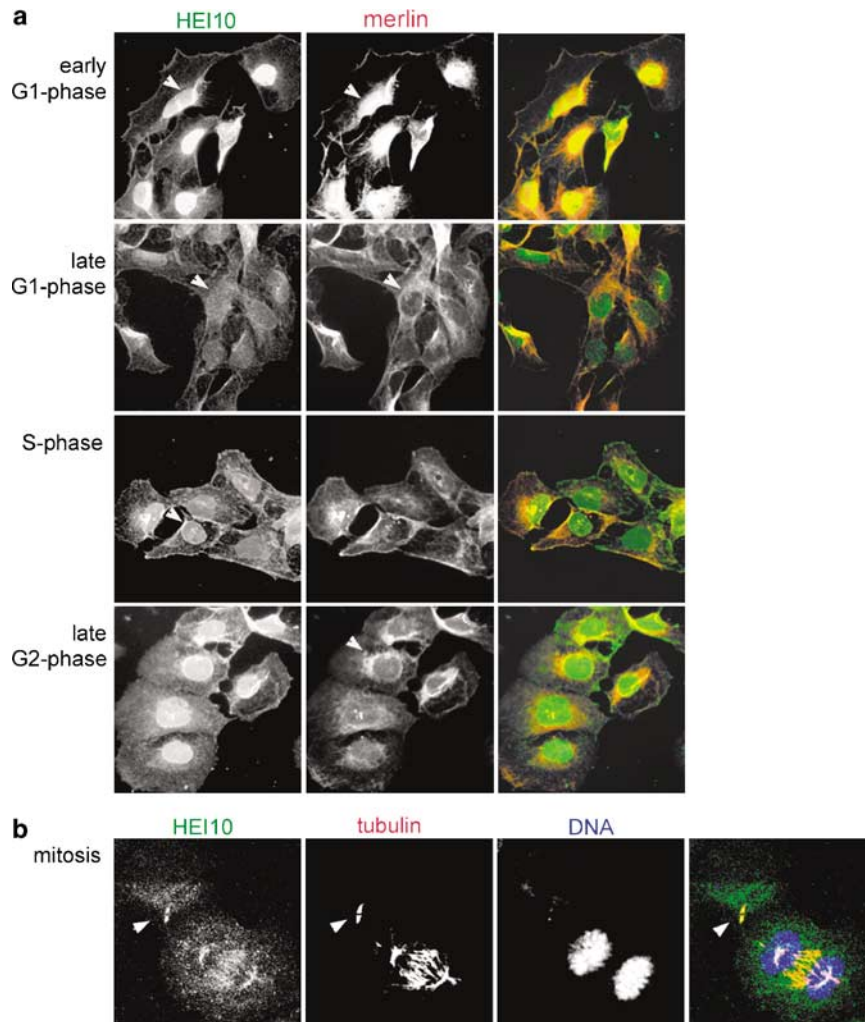


**Figure 5** Localization of merlin and HEI10 at different stages of the cell cycle. (a) U2OS cells were synchronized using nocodazole or mimosine treatment and the block was released. Cells in early and late G1, S and late G2 phase were stained with merlin 1C4 monoclonal antibody (mAb) and HEI10 rabbit antiserum and images taken with an epifluorescence microscope. Nuclear merlin and HEI10 can be seen at early G1 (arrows) after which nuclear merlin and most nuclear HEI10 disappear (arrows). HEI10 shuttles into the nucleus at the onset of S phase (arrow) where it is present until mitosis, while merlin accumulates perinuclearly at late G2 phase (arrow). (b) Mitotic cells were stained with HEI10 rabbit antiserum, tubulin mAb and DAPI to detect DNA and images taken with a confocal microscope. HEI10 can be seen in the mitotic spindle of a dividing cell and the contractile ring in a cell undergoing cytokinesis (arrow).

mainly localized to the submembranous region (Figure 6g).

*The interaction with merlin affects HEI10 protein levels*  
In order to gain insight into the potential functional interplay between merlin and HEI10, 293HEK cells were transfected with HA-HEI10 and merlin constructs 1–595 (wt), 1–547, 1–314 or 492–595, and expression levels of HEI10 and merlin assessed 72 h after transfections (Figure 7a). Similar amounts of HEI10 were detected in cells coexpressing an empty pcDNA3 vector, merlin 1–314 or 492–595. However, cells coexpressing merlin 1–547 demonstrated a significantly reduced amount of HEI10 ( $P=0.0004$ ), and a minor decrease was seen in cells coexpressing merlin 1–595 (wt) ( $P=0.019$ ). Quantification of five experiments indicated

an average 59% reduction of HEI10 in cells coexpressing merlin 1–547 in comparison to control cells, and a 23% reduction in cells coexpressing merlin 1–595 (wt). To study whether binding to merlin is a requirement for the decrease, we tested the merlin 1–547 construct with an insertion at position 307, 1–547/ins307, which abolished HEI10 binding in the yeast two-hybrid experiment. Merlin 1–547/ins307, 1–547 or 1–595 (wt) was co-transfected with HEI10. In contrast to merlin 1–547, which resulted in a significant decrease of the HEI10 protein levels, the effect of 1–547/ins307 on HEI10 protein levels was much weaker, but comparable to that of merlin 1–595 (wt) (Figure 7b), although all merlin constructs were expressed at similar levels.

To study the time dependence of merlin-induced degradation of HEI10, 293HEK cells were transfected with merlin 1–547 and HA-HEI10, and lysed at various

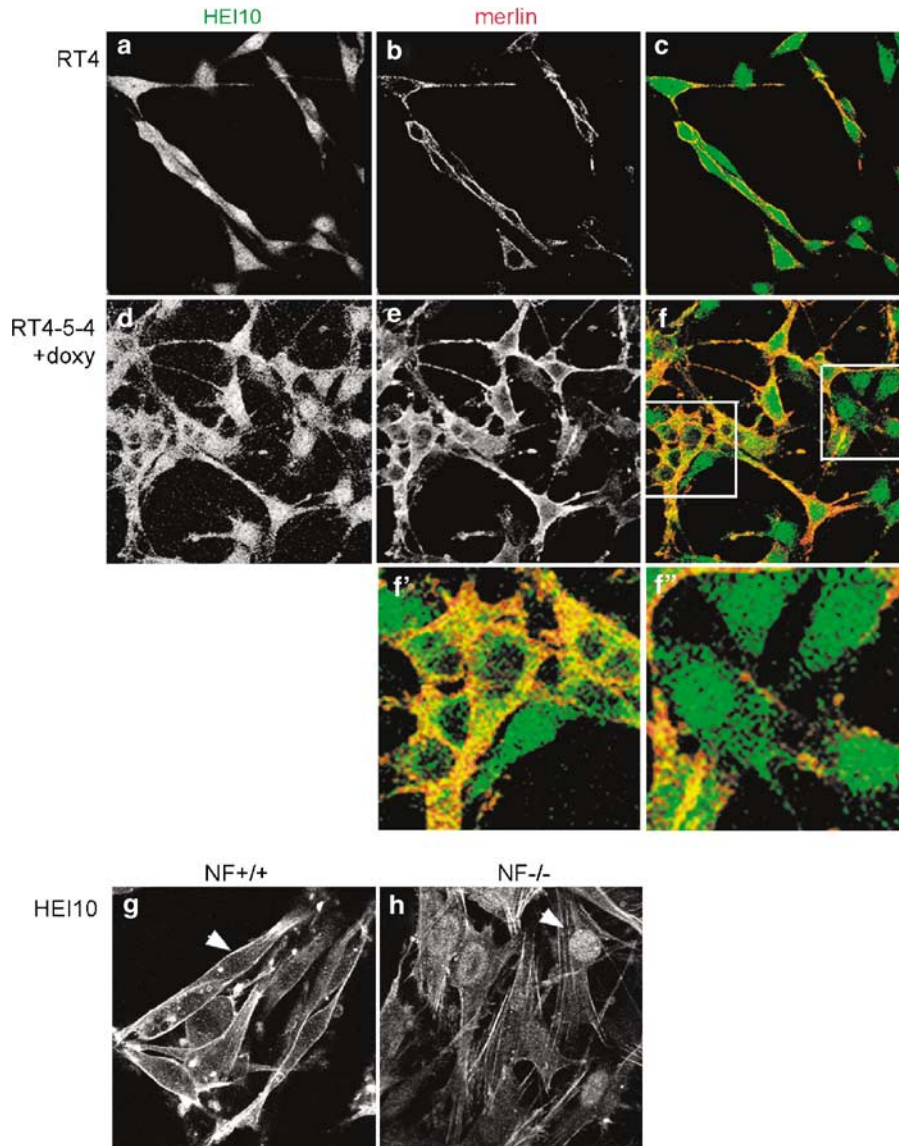


**Figure 6** Expression of merlin changes the subcellular localization of HEI10 in Schwann cell derivatives. RT4 rat schwannoma cells, expressing low amounts of merlin (a–c) and RT4-5-4 schwannoma cells induced to express merlin with doxycyclin (d–f) were stained for merlin with 1C4 monoclonal antibody (mAb) and HEI10 with rabbit antiserum and images taken with a confocal microscope. HEI10 is present in the nucleus of all cells with low merlin expression (c). Cells with high merlin expression are devoid of nuclear HEI10 (f and f'), whereas those RT4-5-4 cells, which express very little merlin, show strong nuclear HEI10 staining (f and f'). Merlin-positive primary human Schwann cells (g) and merlin-negative schwannoma cells (h) were stained for HEI10 with HEI10 rabbit antiserum. Nuclear HEI10 is seen in NF<sup>-/-</sup> cells but not in NF<sup>+/+</sup> cells (arrows).

intervals (Figure 7c). For up to 60 h after transfection, the levels of HA-HEI10 remained constant. However, at 72 and 90 h, a markedly reduced amount of HEI10 was seen, while the level of merlin 1–547 remained unaffected.

In additional experiments, 293HEK cells stably expressing merlin 1–547 or vector only, were transiently transfected with HA-HEI10 or untagged HEI10. Cells were lysed after 60 h, HA-HEI10 detected with anti-HA mAb and untagged HEI10 with the HEI10 rabbit antiserum (Figure 7d). In cells expressing the constitutively open merlin 1–547, the level of HEI10 was reduced compared to empty vector. Interestingly, in these cells a smaller ~22 kDa protein band could be

detected by the HEI10 Ab. This was apparently a degradation product, which was not detected with anti-HA mAb in HA-HEI10-transfected cells.

## Discussion

Resolution of the tumor suppressor mechanism of the *NF2* gene product merlin requires knowledge of its molecular interactions. In this respect, molecules that link merlin to cell cycle regulation are of special interest. In order to find explanations for the opposite effects merlin and ezrin play on cell proliferation we have

focused on molecular interactions that would be specific for either protein. With this approach, we identified the cell cycle regulator HEI10 as a protein that binds merlin but not ezrin.

The interaction, which was verified by yeast two-hybrid, affinity precipitation, and coimmunoprecipitation experiments is mediated between coiled-coil domains on both proteins. Such domains are frequently involved in protein interactions, in particular during protein oligomerization (Burkhard *et al.*, 2001). Interestingly, although the sequence in ezrin is very similar (~90% identity) to the corresponding region in merlin, ezrin does not bind HEI10. Only few interaction

partners are known to bind the alpha-helical part of merlin. One of them is the regulatory subunit RI $\beta$  of PKA (Grönholm *et al.*, 2003). An amphipathic helix disrupting mutation, which inhibits merlin-PKA-RI $\beta$  binding, did not affect HEI10 interaction suggesting that the interactions do not compete with each other. Two NF2 patient missense mutations, L316W and L316F (<http://uwcmmls.uwcm.ac.uk/uwcm/mg/nf2/>, 2005) have been identified within residues 306–339, which is the critical sequence in merlin. These mutations did not, however, affect binding to HEI10, which indicates that disruption of the interaction is not the likely cause of NF2 in these patients. The PAK1 kinase, which is essential for the malignant growth of NF2 gene-deficient cells, is controlled by merlin through two separate binding domains (Hirokawa *et al.*, 2004). Interestingly, the HEI10 binding domain lies within one of them, comprising of amino acids 288–359. Our results also indicate that the association between merlin and HEI10 needs conformational activation of merlin. In yeast two-hybrid and coimmunoprecipitation experiments of transfected 293HEK cells, merlin wt did not bind HEI10. However, merlin 1–547 could be coprecipitated with HEI10 from transfected cells and an N- or C-terminally truncated merlin construct, interacted with HEI10 in the two-hybrid experiment. We have previously shown that N- and C-terminal merlin constructs, including merlin 1–546, mimic an open conformation of merlin, and interact with proteins, which *in vivo* need conformational activation of merlin (Grönholm *et al.*, 1999, 2003). *In vitro* translation-produced merlin 1–595 could be pulled down by GST-HEI10, but this product might not represent the full-length protein, as the C-terminus of recombinant ERM proteins is easily degraded, and such degradation results in loss of the

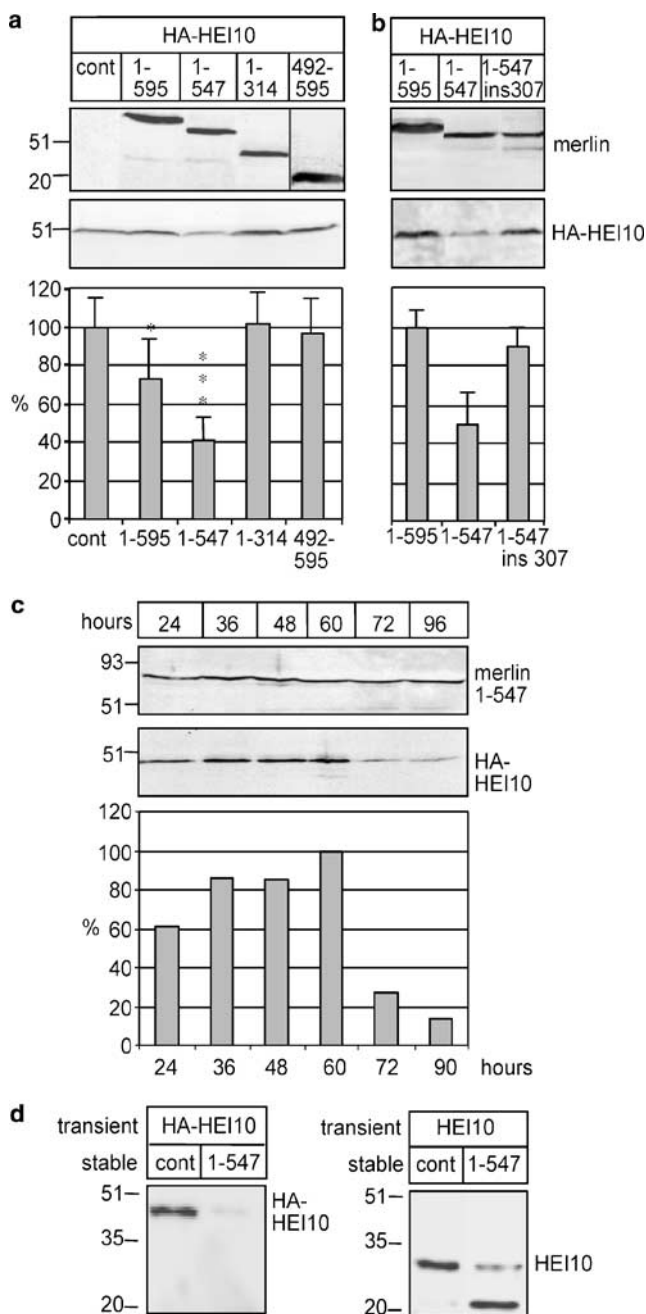


**Figure 7** Constitutively open merlin regulates HEI10 protein levels. (a) 293HEK cells were transiently transfected with HA-HEI10 and different merlin constructs or an empty pcDNA3 vector (cont). Cells were lysed after 72 h, samples normalized for protein concentration, and detected with A19 rabbit antiserum for N-terminal merlin constructs, C18 to detect merlin 492–595, anti-HA monoclonal antibody (mAb) to detect HA-HEI10 (~45 kDa) and HEI10 rabbit antiserum to detect untagged HEI10 (32 kDa). In cells expressing merlin 1–547 and 1–595 (wt) a decreased amount of HEI10 can be seen. The bottom panel shows quantified intensity of the HEI10 band in cells expressing various merlin constructs. Mean values and standard deviation of five experiments. Bars represent percentage compared to control cells (100%). \* $P < 0.05$ , \*\*\* $P < 0.01$ . (b) The same experiment as above performed with merlin 1–547 with a five amino-acid insertion at position 307, 1–547/ins307. Less decrease in the HEI10 amount could be seen with this construct. Bars represent percentage compared to merlin 1–595 (100%). \*\*\* $P < 0.01$ . (c) 293HEK cells co-transfected with HA-HEI10 and merlin 1–547 were lysed after 24, 36, 48, 60, 72 and 96 h and detected as above. Bars represent percentage compared to the highest expression level at 60 h (100%). (d) The same experiment as in A was performed with cells stably expressing merlin 1–547 or empty vector and transiently transfected with HA-HEI10 or untagged HEI10. A decrease of the ~45 kDa HA-HEI10 band can be seen with the anti-HA mAb and of the HEI10 32 kDa band with the HEI10 rabbit antiserum. An additional band around 22 kDa can be seen with the HEI10 rabbit antiserum but not with anti-HA mAb.

intramolecular bond between N- and C-terminus (Chambers and Bretscher, 2005).

Many of the known tumor suppressors undergo nucleo-cytoplasmic shuttling as an efficient, simple and rapid way to control cell growth (Fabbro and Henderson, 2003). Merlin is typically localized to cortical actin structures in patterns that partly overlap with ERM proteins (Gonzalez-Agosti *et al.*, 1996; Sainio *et al.*, 1997; Shaw *et al.*, 1998). However, it can also be targeted to the nucleus dependent on the cell cycle phase, cell density and adhesive state (Muranen *et al.*, 2005). In this study we show that also HEI10 localizes to the nucleus in a cell cycle-dependent manner and to the cortical actin cytoskeleton. The partial colocalization between merlin and HEI10 can indicate functional interplay between merlin and HEI10 in certain cell cycle phases. Nucleo-cytoplasmic shuttling may provide means for merlin and HEI10 to affect cell growth, although no nuclear function for either protein has been identified yet.

In a recent report, expression of merlin in a *NF2* gene-deficient mesothelioma cell lines caused accumulation of cells in G1 concomitant with a decreased expression of cyclin D1, inhibition of Cdk4 activity and dephosphorylation of Rb, which are important steps for G1/S transition. This decrease was caused by merlin's inhibitory effect on PAK, a known upstream activator of cyclin D1 transcription (Xiao *et al.*, 2005). The current results link merlin to cyclin B and thus to another control point of the cell cycle. Further studies are needed to find out, whether the pathways are regulated independently or in parallel.

Schwannomas are the primary manifestation of NF2. Therefore, it is of interest that Schwann cells express HEI10 and that its distribution depends on the expression of merlin. In human and rat schwannoma cells deficient for merlin expression, HEI10 was targeted to the nucleus, whereas in human Schwann cells and in rat schwannoma cells expressing increased levels of merlin, HEI10 was cytoplasmic. The results indicate that merlin is, either directly or indirectly, involved in targeting of HEI10. An indirect effect might result from the fact that merlin expressing cells are more frequently in G1 than merlin-negative cells (Schulze *et al.*, 2002), and during G1 HEI10 was shown to have mainly cytoplasmic location. Since both proteins are exported from the nucleus at a similar time frame during G1, it is also possible that merlin contributes to the transport of HEI10 from the nucleus. Our interpretation is that in cells deficient for merlin, the function of HEI10 is compromised due to inappropriate targeting.

Interestingly, the constitutively open form of merlin affected the integrity of the HEI10 protein. Coexpression of merlin 1–547 with HEI10 resulted in degradation of HEI10 with a mechanism that required binding between the two proteins. The mechanism of degradation is not yet clear. HEI10 can be ubiquitinated and can function as an E3 ubiquitin ligase (Toby *et al.*, 2003). However, preliminary experiments with proteasome inhibitors did not affect the degradation induced by constitutively open merlin.

Previously, models for the tumor suppressor role of merlin at the membrane-cytoskeleton interphase have been proposed. We have shown a more versatile localization of merlin, which is regulated by cell cycle phase, and demonstrate here an association between merlin and the cell cycle regulator. This suggests that merlin performs several functions in cells, which may all be linked to its function as a tumor suppressor.

## Materials and methods

### *Antibodies and probes*

1C4 mAb (Gonzalez-Agosti *et al.*, 1996), KF10 mAb (den Bakker *et al.*, 1995) and A19 or C18 rabbit antiserum (Santa Cruz Biotechnology Inc., Santa Cruz, CA, USA) were used to detect merlin. The anti-HEI10 antibody has been described (Toby *et al.*, 2003). In addition, we used anti-HA antibody (Covance Inc., Princeton, NJ, USA), anti- $\alpha$ -tubulin mAb N356 (Amersham Pharmacia Biotech, Buckinghamshire, UK), DAPI to stain DNA (Sigma, St Louis, MO, USA) and propidium iodide (Sigma).

### *Cell cultures and stainings*

U2OS human osteosarcoma cells were cultured in McCoy's medium supplemented with 15% fetal bovine serum, and 293HEK cells in RPMI medium with 10% FBS and RT4 and RT4-5-4 rat schwannoma cells (Morrison *et al.*, 2001) in DMEM medium with 10% FBS. Expression of merlin in RT4-5-4 cells was induced by 1  $\mu$ g/ml doxycycline (Orion Pharma, Espoo, Finland) for 24 h. Since merlin expression affects RT4-5-4 cell proliferation in confluent cells (Morrison *et al.*, 2001), cells were not allowed to grow to confluency. 293HEK cultures stably expressing full-length merlin (1–595, wt), merlin 1–547 or empty pcDNA3 vector (Invitrogen, Carlsbad, CA, USA) were produced by selection in 100  $\mu$ g/ml hygromycin (Gibco). Cells were fixed in 3.5% paraformaldehyde (PFA), pH 7.4, and stained with 1C4 mAb (1:100) or A19 rabbit antiserum (1:200) to detect merlin and with anti-HEI10 rabbit antiserum (1:50) to detect HEI10 followed by Alexa488 anti-mouse or Alexa594 anti-rabbit antibodies (Molecular Probes, Eugene, OR, USA). Coverslips were mounted in DABCO (Sigma) and Mowiol (Calbiochem, San Diego, CA, USA) and examined by confocal microscopy (Leica SP2, Leica Microsystems, Heerbrugg, Switzerland) using the sequential scanning mode, or by immunofluorescence microscopy (Zeiss Axiophot epifluorescence microscope equipped with AxioCam cooled CCD-camera, Carl Zeiss, Esslingen, Germany).

Normal human Schwann and schwannoma cells were isolated as previously described (Hanemann *et al.*, 1998; Rosenbaum *et al.*, 1998). Following collection, cells were resuspended in proliferation medium (DMEM, 10% fetal calf serum, 500 U/ml penicillin/streptomycin (Gibco), 0.5  $\mu$ M forskolin (Sigma), 10 nM  $\beta$ 1-herectulin177–244 (Mark Sliwkowski, Genentech, San Francisco, CA, USA), 0.5 mM 3-isobutyl-1-methylxanthine (Sigma), 2.5  $\mu$ g/ml insulin (Sigma)). Cells were seeded on plates pre-coated with 1 mg/ml poly-L-lysine (Sigma) and 4  $\mu$ g/ml natural mouse laminin (Gibco). Cells were fixed by 4% PFA, permeabilized with 0.2% Triton X-100 for 5 min and blocked in 10% goat serum/1% bovine serum albumin in phosphate-buffered saline, before incubation with the HEI10 rabbit antiserum overnight at 4°C and goat-anti-rabbit Cy3 1:800 (Dianova) for 40 min. Cells were analysed on a confocal scanning microscope (LSM510, Leica), and experiments were repeated three times using cell cultures from different donors each.

#### Production of glutathione S-transferase-fusion proteins

Glutathione S-transferase-fusion proteins were expressed in *Escherichia coli* (DH5 $\alpha$ ) and purified following standard protocols. Fusion proteins were eluted from glutathione-Sepharose (G-Sepharose) beads by 5 mM reduced glutathione in 50 mM Tris-HCl, pH 8 over night at 4°C.

#### In vitro translation

Merlin pcDNA3 plasmids were used as a template for a T7-coupled rabbit reticulocyte transcription-translation system (Promega, Madison, WI, USA) in the presence of <sup>35</sup>S-methionine (Sigma). Of 50  $\mu$ l reaction, 5  $\mu$ l were separated in SDS-PAGE, the gel was dried and exposed on film to determine the size and amount of labelled protein. Fusion proteins on glutathione beads (~1  $\mu$ g) were mixed with IVT-produced protein. Bound proteins were separated in SDS-PAGE, and detected with autoradiography.

#### Affinity precipitation

Yeast expressing HA-tagged merlin constructs were lysed with a mini beadbeater (BioSpec Products Inc., Bartlesville, OK, USA) in the presence of 1 ml acid-washed glass beads (Sigma) in 200  $\mu$ l of ELB-buffer (50 mM Hepes, pH 7.4, 150 mM NaCl, 5 mM EDTA), 1% NP-40 and protease inhibitors. Debris was removed by centrifugation, and supernatant diluted to ELB-0.5% NP-40. Total protein (200  $\mu$ g) from lysates were incubated with purified GST-fusion protein bound to G-Sepharose beads (0.5–1  $\mu$ g) for 45 min. Beads were washed in ELB-0.1% NP-40 buffer and bound proteins eluted by boiling in non-reducing Laemmli sample buffer, separated in SDS-PAGE and analysed by immunoblotting. Bound proteins were detected with anti-HA antibody (1:3000).

#### Yeast two hybrid

A yeast two-hybrid screen was performed with merlin amino acids 252–595 cloned in the EG202 vector as bait using a HeLa cDNA library in the JG4-5 vector as described (Gyuris *et al.*, 1993). Merlin, ezrin and HEI10 constructs were cloned into EG202 and JG4-5 vectors. Mutations were introduced in merlin constructs using the QuickChange Kit (Stratagene, La Jolla, CA, USA) and their authenticity verified by sequencing. Yeast two-hybrid mating assays and detection of interactions were performed as described (Grönholm *et al.*, 1999). Identification of the merlin coiled-coil domain was performed with COILS-prediction program ([www.ch.embnet.org/software/COILS\\_form.html](http://www.ch.embnet.org/software/COILS_form.html)).

#### Merlin transposon mutation library

Merlin mutation library with random pentapeptide insertions was constructed in the yeast two-hybrid vector pYesTrp2 (Invitrogen) containing merlin 1–546 using an *in vitro* DNA transposition-based peptide insertion mutagenesis system (Finnzymes Oy, Espoo, Finland). The library was transformed

into yeast and interaction with HEI10 1–200 in the EG202 vector tested with the yeast two-hybrid mating assay (Grönholm *et al.*, 1999).

#### Cell transfections and Western blot analysis

293HEK cells were grown as above and transfected with a pcDNA3 vector expressing HA-HEI10, which contains 6 inserted HA-tags adding ~90 amino acids to the expressed protein, or untagged HEI10 and different pcDNA3/merlin constructs using the Fugene transfection reagent (Roche, Mannheim, Germany). Transfected subconfluent cells were lysed after 24–90 h in 500  $\mu$ l ELB-buffer (50 mM Hepes, pH 7.4, 150 mM NaCl, 5 mM EDTA), supplemented with 0.5% NP-40, protease and phosphatase inhibitors, and lysates normalized for protein concentration. Samples were separated in SDS-PAGE and analysed by immunoblotting using the anti-HA antibody (1:3000), HEI10 rabbit antiserum (1:50) or merlin A19 rabbit antiserum (1:1500). Proteins were detected with enhanced chemiluminescence. Western blot bands from five different experiments were analysed using the Image J imaging program and the mean values and standard deviation calculated.

#### Coimmunoprecipitation

293HEK cells stably expressing merlin 1–595 (wt), 1–547 or empty vector were transfected with the pcDNA3/HA-HEI10 construct, and lysed as above. Lysates were centrifuged at 15 000 *g* for 1 h at 4°C. The supernatant was incubated with KF10 mAb, anti-HA mAb or X63, together with protein G-Sepharose beads (Amersham Biosciences, Uppsala, Sweden) for 4 h at 4°C. Immunoprecipitates were washed with ELB-0.1% NP-40 and bound proteins were eluted from the beads by boiling in non-reducing Laemmli sample buffer. Precipitated proteins were detected as above.

#### Cell cycle studies

For cell cycle synchronization, U2OS cells were treated with nocodazole (200–400 ng/ml, Calbiochem) or L-mimosine (200–400  $\mu$ M, Calbiochem). After 18–24 h, the block was released. At various time points after release, samples were taken for immunofluorescence analysis as described.

#### Acknowledgements

We thank V Ramesh for the merlin 1C4 mAb, L Sherman for the RT4 and RT4-5-4 cell lines, and H Ahola, S Blomqvist, T Halmesvaara, A Partanen and M Schoultz for skillful technical assistance. This work was supported by United States Army Neurofibromatosis Research Grant DAMD17-00-0550, The Finnish Cancer Society, the Pennsylvania Tobacco Settlement Fund, Finsk-Norska Medicinska Stiftelsen and Svenska kulturfonden.

#### References

- Alfthan K, Heiska L, Grönholm M, Renkema GH, Carpen O. (2004). *J Biol Chem* **279**: 18559–18566.
- Arakawa H, Hayashi N, Nagase H, Ogawa M, Nakamura Y. (1994). *Hum Mol Gen* **3**: 565–568.
- Bretscher A, Edwards K, Fehon RG. (2002). *Nat Rev Mol Cell Biol* **3**: 586–599.
- Burkhard P, Stetefeld J, Strelkov SV. (2001). *Trends Cell Biol* **11**: 82–88.
- Chambers DN, Bretscher A. (2005). *Biochemistry* **44**: 3926–3932.
- den Bakker MA, Tascilar M, Riegman PH, Hekman AC, Boersma W, Janssen PJ *et al.* (1995). *Am J Pathol* **147**: 1339–1349.
- Fabbro M, Henderson BR. (2003). *Exp Cell Res* **282**: 59–69.
- Geiger KD, Stoldt P, Schlote W, Derouiche A. (2000). *Am J Pathol* **157**: 1785–1793.
- Gonzalez-Agosti C, Wiederhold T, Herndon ME, Gusella J, Ramesh V. (1999). *J Biol Chem* **274**: 34438–34442.
- Gonzalez-Agosti C, Xu L, Pinney D, Beauchamp R, Hobbs W, Gusella J *et al.* (1996). *Oncogene* **13**: 1239–1247.

- Grönholm M, Sainio M, Zhao F, Heiska L, Vaheri A, Carpén O. (1999). *J Cell Sci* **112**: 895–904.
- Grönholm M, Vossebein L, Carlson CR, Kuja-Panula J, Teesalu T, Alftan K *et al.* (2003). *J Biol Chem* **278**: 41167–41172.
- Gutmann DH, Sherman L, Seftor L, Haipek C, Hoang Lu K, Hendrix M. (1999). *Hum Mol Genet* **8**: 267–275.
- Gyuris J, Golemis E, Chertkov H, Brent R. (1993). *Cell* **75**: 791–803.
- Hanemann CO, Rosenbaum C, Kupfer S, Wosch S, Stoegbauer F, Muller HW. (1998). *Glia* **23**: 89–98.
- Hirokawa Y, Tikoo A, Huynh J, Utermark T, Hanemann CO, Giovannini M *et al.* (2004). *Cancer J* **10**: 20–26.
- Huynh DP, Pulst SM. (1996). *Oncogene* **13**: 73–84.
- Ilmonen S, Vaheri A, Asko-Seljavaara S, Carpén O. (2005). *Mod Pathol* **18**: 872.
- Khanna C, Wan XL, Bose S, Cassaday R, Olomu O, Mendoza A *et al.* (2004). *Nat Med* **10**: 182–186.
- Kissil JL, Johnson KC, Eckman MS, Jacks T. (2002). *J Biol Chem* **277**: 10394–10399.
- Louis DN, Ramesh V, Gusella JF. (1995). *Brain Pathol* **5**: 163–172.
- Lutchman M, Rouleau GA. (1995). *Cancer Res* **55**: 2270–2274.
- Mäkitie T, Carpén O, Vaheri A, Kivelä T. (2001). *Invest Ophthalmol Vis Sci* **42**: 2442–2449.
- McClatchey AI. (2003). *Nat Rev Cancer* **3**: 877–883.
- Mine N, Kurose K, Konishi H, Araki T, Nagai H, Emi M. (2001). *Jpn J Cancer Res* **92**: 135–139.
- Morrison H, Sherman LS, Legg J, Banine F, Isacke C, Haipek CA *et al.* (2001). *Gene Dev* **15**: 968–980.
- Muranen T, Grönholm M, Renkema GH, Carpén O. (2005). *Oncogene* **24**: 1150–1158.
- Pineau P, Marchio A, Cordina E, Tiollais P, Dejean A. (2003). *Int J Cancer* **106**: 216–223.
- Rosenbaum C, Kluwe L, Mautner VF, Friedrich RE, Muller HW, Hanemann CO. (1998). *Neurobiol Dis* **5**: 55–64.
- Sainio M, Zhao F, Heiska L, Turunen O, den Bakker M, Zwarthoff E *et al.* (1997). *J Cell Sci* **110**: 2249–2260.
- Schulze KM, Hanemann CO, Muller HW, Hanenberg H. (2002). *Hum Mol Genet* **11**: 69–76.
- Shaw RJ, McClatchey AI, Jacks T. (1998). *J Biol Chem* **273**: 7757–7764.
- Sherman L, Xu HM, Geist RT, Saporito-Irwin S, Howells N, Ponta H *et al.* (1997). *Oncogene* **15**: 2505–2509.
- Smith AP, Weeraratna AT, Spears JR, Meltzer PS, Becker D. (2004). *Cancer Biol Ther* **3**: 104–109.
- Toby GG, Gherraby W, Coleman TR, Golemis EA. (2003). *Mol Cell Biol* **23**: 2109–2122.
- Tynninen O, Carpén O, Jääskeläinen J, Paavonen T, Paetau A. (2004). *Neuropathol Appl Neurobiol* **30**: 472–477.
- Xiao GH, Beeser A, Chernoff J, Testa JR. (2002). *J Biol Chem* **277**: 883–886.
- Xiao GH, Gallagher R, Shetler J, Skele K, Altomare DA, Pestell RG *et al.* (2005). *Mol Cell Biol* **25**: 2384–2394.

**The tumor suppressor merlin interacts with microtubules and modulates Schwann cell microtubule cytoskeleton**

Taru Muranen<sup>1</sup>, Mikaela Grönholm<sup>1</sup>, Aurelie Lampin<sup>2</sup>, Dominique Lallemand<sup>2</sup>, Fang Zhao<sup>1</sup>, Marco Giovannini<sup>2</sup> and Olli Carpén<sup>1,3</sup>.

<sup>1</sup>Biomedicum Helsinki, Program of Neuroscience, Department of Pathology, 00014 University of Helsinki, Finland.

<sup>2</sup>Inserm U674, Fondation Jean Dausset-CEPH et Institut Universitaire d'Hématologie, 75010 Paris, France.

<sup>3</sup>Department of Pathology, University of Turku and Turku University Central Hospital, 20520 Turku, Finland.

Corresponding author: Taru Muranen

E-mail: [Taru.Muranen@helsinki.fi](mailto:Taru.Muranen@helsinki.fi)

Tel: +358919125651

Fax: +358947171964



## **Abstract**

The lack of Neurofibromatosis 2 tumor suppressor protein merlin leads to formation of nervous system tumors, specifically schwannomas and meningiomas. Merlin is considered to act as a tumor suppressor at the cell membrane, where it links transmembrane receptors to actin cytoskeleton. Several tumor suppressors interact with microtubules in a regulated manner and control microtubule dynamics. In this work, we have identified merlin as a novel microtubule organizing protein. Two tubulin-binding sites were identified in merlin, one residing at the N-terminal FERM-domain and another at the C-terminal domain. Merlin's intramolecular association and phosphorylation of serine 518 regulate the interaction between merlin and tubulin. Analysis of cultured cells indicates that colocalization between merlin and microtubules depends on cell cycle stage; in synchronized cells merlin and tubulin colocalize only during mitosis at the mitotic spindles and during cytokinesis at the midbody. In addition, in primary mouse Schwann cells the two proteins colocalize at the cell membrane. Loss of merlin in cultured Schwann cells drastically alters their microtubule cytoskeleton. Both *in vitro* assays and *in vivo* studies in Schwann cells indicate that merlin promotes tubulin polymerization. The results indicate that merlin plays a key role in the regulation of Schwann cell microtubule cytoskeleton and suggest a mechanism by which loss of merlin leads to cytoskeletal defects observed in human schwannomas.

Words: 216

## **Introduction**

Inactivation of the neurofibromatosis 2 (*NF2*) tumor suppressor gene leads to development of multiple benign tumors of the nervous system, in particular meningiomas and bilateral schwannomas, Schwann cell-derived tumors of the eighth cranial nerve (1). The *NF2* gene encodes a 595-amino acid protein merlin (schwannomin), which is related to the ezrin-radixin-moesin (ERM) protein family. Merlin and ERM proteins are located primarily underneath the cell membrane where they anchor transmembrane proteins to actin cytoskeleton (2,3). ERM proteins and merlin form homo- and heterotypic interactions (4) and these interactions can regulate the functions of ERM-proteins and their interactions with most of the other proteins (5,6,7). Head-to-tail binding leads to a closed conformation of the ERM proteins (4); for merlin, the closed form is thought to act as a tumor suppressor, whereas an open protein is considered to be unable to regulate growth. Phosphorylation of a C-terminal serine (S518) by the p21 activated kinases (PAK's) or cAMP dependent protein kinase A (PKA) weakens merlin's self-association and is believed to inactivate the growth suppressing activity of merlin (8,9). However, the functional regulation of merlin is still incompletely understood.

Merlin has also been shown to be involved in receptor recycling and endocytosis. It inhibits PDGFR degradation (10) and binds hepatocyte growth factor-regulated tyrosine kinase substrate (HRS) (11), which is known to regulate receptor tyrosine kinase trafficking to the degradation pathway (12). Recently merlin was shown to regulate EGF receptor recycling and turnover in *Drosophila* (13). Thus, increasing evidence is positioning merlin to the membrane where it can bind membrane receptors and regulate their expression and localization.

Microtubules are known to regulate cell growth. For instance, microtubules control cell division and regulate endocytosis and recycling of growth factor receptors (14). In addition, a common feature of many tumor suppressors is their ability to interact with microtubules and regulate microtubule stability (15,16). We set out to study merlin tubulin interaction after we saw endogenous merlin to colocalize with tubulin in mitotic structures of U251 cells (17). Even though merlin has previously been suggested to bind

tubulin *in vitro* (3,18), no further evidence has been provided to support the binding. Here we have studied the association between merlin and tubulin; the effects merlin has on microtubule dynamics, and the consequences of loss of merlin on microtubule system in Schwann cells. Our results show that merlin plays an important role in regulating microtubule cytoskeleton of mouse primary Schwann cells.

## **Results**

### **Merlin associates with microtubules**

Previous work from our lab shows that in synchronized U251 glioma cells merlin localizes to mitotic structures (17,19). This led us to analyze the distribution of endogenous merlin and tubulin at various cell cycle stages in U251 cells (Fig. 1 a-i). We noticed parallel accumulation of merlin and tubulin around the nucleus at cells preparing for mitotic division (a). During mitosis, merlin colocalized with microtubules at the mitotic spindles, although some diffuse merlin staining was also noticed in the cytoplasm (b-c, i). During cytokinesis especially the midbody demonstrated high degree of colocalization between merlin and tubulin (d-e). The colocalization was lost at early G1, in which merlin accumulated in the nucleus while tubulin was cytoplasmic (f). The staining patterns remained separate during the entire G1 and S phase (g). At late G2, the proteins started to colocalize again (h). Unlike in U251 cells, in primary mouse Schwann cells merlin and tubulin colocalized also in interphase cells, the colocalization being most apparent beneath the plasma membrane (j-m). This colocalization is also dependent on cell confluency. In confluent Schwann cell cultures (j-k) the colocalization was more readily detected than in subconfluent cultures (l-m).

### **Merlin binds polymerized microtubules *in vitro***

Next we wanted to identify the tubulin binding regions in merlin. We mapped the interaction sites with tubulin pull-down assay using various purified GST-merlin constructs (Fig 2A). Both the N-terminal FERM- (aa 1-314) and the C-terminal (aa 492-595) domain were recovered from the tubulin pellet whereas the  $\alpha$ -helical region (aa 314-492) of merlin or GST alone (not shown) did not bind tubulin (Fig. 2B). We further

mapped the N-terminal binding site to amino acids 1-100 and the C-terminal binding site to residues 492-537 (Fig 2C). In addition we produced *in vitro* translated methionine-labeled merlin and pulled it down with polymerized tubulin. With this assay we saw an interaction between tubulin and merlin isoforms I and II (Fig. 2C). C-terminal deletion constructs 1-569 and 1-587 bound tubulin similarly to isoform I. On the other hand 1-547 (1-547 construct was used since truncations in this region are found in NF2 patients, <http://neurosurgery.mgh.harvard.edu/NFclinic/NFresearch.htm>) showed reduced binding in comparison to isoform I, whereas a further truncation of 10 residues returned the binding activity (Fig 2D). A similar result was seen with recombinant GST-fusion proteins (Fig 2C).

### **Intramolecular association and phosphorylation of merlin regulate its binding to microtubules**

Merlin has been shown to undergo conformational regulation and is capable of forming an intramolecular association between its N- and C-terminal domains (6). This intramolecular association can mask many of the binding sites in merlin. Therefore we studied whether intramolecular binding affects merlin-tubulin binding. Purified C-terminal GST-merlin was incubated together with increasing concentrations of the N-terminus in order to saturate the C-terminal binding site. When C-terminus was saturated it could no longer bind to tubulin and *vice versa* (Fig 3A). Plain GST incubated with the C-terminus was used as a negative control. From this data we concluded that the intramolecular interaction is able to inhibit merlin-tubulin binding.

The C-terminal S518 of merlin can be phosphorylated by p21 activated kinases and cAMP dependent protein kinase A (8,9,20). This phosphorylation is thought to affect merlin's growth-regulating activity (21,22,23). We wanted to study whether the C-terminal phosphorylation has an effect on merlin-tubulin binding. We phosphorylated the C-terminus of GST-merlin *in vitro* with PKA and performed the tubulin pull-down assay (Fig 3B). Phosphorylation was verified by a <sup>32</sup>P ATP labeling (not shown). Significantly lower amount of merlin was pulled down after PKA treatment indicating that the phosphorylation of the serine 518 decreases the binding of merlin to tubulin *in vitro*.

### **Merlin enhances microtubule polymerization *in vitro***

Many tumor suppressor proteins affect tubulin polymerization (15); therefore we studied whether merlin has an effect on tubulin polymerization. Purified tubulin was polymerized *in vitro* and the polymerization was monitored at OD<sub>350</sub>. When merlin was added to the polymerization reaction, the rate of tubulin polymerization was increased (Fig 4A). This effect was dependent on the concentration of merlin (Fig 4B). Interestingly, merlin 1-547, which has reduced affinity to tubulin, was unable to induce tubulin polymerization.

### **Microtubule cytoskeleton of Schwann cells lacking merlin**

Schwannomas, the hallmark of Neurofibromatosis 2, originate from Schwann cells. Therefore, it was of interest to study merlin's effect on microtubule cytoskeleton in this cell type. We used primary mouse Schwann cells lacking merlin (NF2 $\Delta$ exon2) and re-introduced wild type merlin via adenovirus infection. The microtubule cytoskeleton of the NF2 $\Delta$ exon2 mouse Schwann cells (NF2 $-/-$ ) differed markedly from cells expressing merlin (NF2 add-back). In the NF2 add-back cells microtubules were assembled as dense cables reaching from one end of the cell to the other and the cells displayed a normal spindle-like structure (Fig 5A). Instead, the microtubules of the NF2  $-/-$  cells were disorganized, and the overall cell shape was more spread (Fig 5B). Similar morphological differences have also been described in cultured human Schwann cells vs. schwannoma cell (39).

The amount of polymerized vs. unpolymerized (*i.e.* soluble) tubulin was analyzed from cells extracted with Triton X-100. More soluble  $\alpha$ - and  $\beta$ -tubulin was present in the NF2  $-/-$  cells than in wild-type cells (Fig 5C). The amount of soluble tubulin was associated with the expression level of merlin, increasing merlin expression resulting in reduced soluble tubulin. The total amount of tubulin in NF2  $-/-$  and the add-back Schwann cells was evaluated after solubilization in 6M Urea buffer. When the Urea-lysates were analyzed in SDS-PAGE the add-back cells appeared to contain at least equal amount of tubulin as the NF2  $-/-$  cells. From this data we conclude that the ratio of polymerized/unpolymerized tubulin differs between NF2  $-/-$  and add-back cells; the

primary NF2 *-/-* Schwann cells express more tubulin ( $\alpha/\beta$ ) that is not associated with the microtubule polymers.

The difference in the integrity of the tubulin cytoskeleton in the Schwann cells led us to test whether a difference in the polymerization rates of tubulin is seen also *in vivo*. We treated the cells with Nocodazole, which sequesters tubulin monomers and thereby depolymerizes microtubules. Incubation with Nocodazole reversed the normal morphology of Schwann cells and the cells obtained a more fibroblast-like morphology (Fig 6A, 0 min). Twenty minutes after the release of Nocodazole block wild type cells began to regain their normal morphology and simultaneously organized microtubule structures were seen, whereas the NF2 *-/-* cells did not have their normal morphology even after two hours of the block release. This implies that the normal Schwann cell morphology is dependent on intact microtubule cytoskeleton and that merlin enhances microtubule polymerization in the Schwann cells.

We used fluorescence recovery after photobleaching (FRAP) technology to study, whether tubulin kinetics were altered in primary Schwann cells lacking merlin. Schwann cells were transfected with GFP-tubulin and 24 hours after transfection the cells were analyzed by FRAP. Cells expressing merlin had a faster recovery rate of tubulin than the NF2 *-/-* cells (Fig. 6B). Within the 20 first seconds after photobleaching, cells expressing wild-type merlin had a 25% faster recovery rate of tubulin than NF2 *-/-* cells. ( $p < 0.001$ ). The data suggest that merlin is able to enhance microtubule dynamics in Schwann cells *in vivo*.

## **Discussion**

In this study we describe a novel function for merlin as a regulator of microtubule organization and dynamics. We show that merlin directly binds tubulin and that it can regulate microtubule dynamics *in vitro* and *in vivo*. We show that merlin and tubulin colocalize in centrosomes during mitosis and partial colocalization is also seen under the cell membrane of interphase Schwann cells. Merlin belongs to the family of FERM-

domain (4.1-*ezrin-radixin-moesin*) proteins (24). Previously, another family member, protein 4.1, was shown to localize to centrosomes, and some isoforms of this protein were shown to disturb the microtubule cytoskeleton in the *Xenopus* extracts (25).

The results indicate that merlin contains two tubulin-binding sites, one in the FERM-domain and another in the C-terminal domain. The existence of two separate binding sites in merlin indicates that merlin could bind either laterally to the sides of the microtubules or by cross-linking individual microtubules to each other, this way 'bundling' the microtubules to thicker entities. Both binding sites appear to be required, as the deletion construct merlin 1-547, which has a reduced binding activity, was not able to induce tubulin polymerization. An intramolecular association and phosphorylation of S518 in merlin can regulate the binding to microtubules. The binding of several other proteins to microtubules is regulated by phosphorylation. For example a major phosphoprotein in the brain, microtubule associated protein 2 (MAP2), is phosphorylated by PKA and upon phosphorylation dissociates from microtubules (26). MAP2 and merlin both function as protein kinase A-anchoring proteins (AKAP's) (27,28), therefore merlin might have a similar function with MAP2, targeting PKA to microtubules. In addition PKA also phosphorylates merlin (9) and is able to modify microtubule dynamics and organization in mitosis (29). Also PAK, shown to phosphorylate merlin at S518 (8,20), localizes to centrosomes and affects microtubule formation (30). It is of interest that the machinery known to regulate phosphorylation of merlin localizes to the centrosomes at mitosis, in analogy with merlin. Previously it has been reported that phosphorylation of merlin results in conformational opening of the molecule (23). However, in light of our study it seems that the regulation is more complex than previously thought. We hypothesize that there is a state where merlin is open but dephosphorylated at S518 since our data shows that only the open but S518 dephosphorylated merlin is able to bind tubulin.

Our data implies that merlin plays an important role in regulating Schwann cell microtubule cytoskeleton. The overall spindle-like cell shape disappears when merlin is removed from these cells and the normal organization of microtubules is altered. It also seems that the ratio of polymerized and unpolymerized tubulin is affected by merlin, *i.e.*

Schwann cells that lack merlin have more unpolymerized tubulin than cells expressing merlin. The NF2  $-/-$  cells contain more acetylated tubulin, which is usually a marker of older and more stable structures. This might imply that tubulin polymerization/turn-over is not as efficient in the NF2  $-/-$  cells as in merlin-expressing cells. Our FRAP data supports this finding; it appears that tubulin turnover is higher in merlin-expressing Schwann cells. The results from the Nocodazole-repolymerization experiment further confirm these data; tubulin polymerization is much slower in the NF2  $-/-$  cells. Unfortunately, in our experimental FRAP setup, it was not possible to monitor the dynamics of individual microtubules due to the thickness of the cells and due to the high amount of free tubulin dimers. Therefore, by FRAP we have only analyzed tubulin recovery as a tubulin pool and not as microtubule polymers. The difference might have been even greater if we had been able to study individual microtubule polymers. It also seems that microtubules are a major contributor to the Schwann cell morphology as after depolymerization of microtubules Schwann cell morphology resembled that of fibroblasts.

Microtubules regulate endocytic pathways (31). A recent paper by Maitra et al. (2006) links also merlin to endocytic events (13). They noticed that insect cells expressing mutant merlin together with mutant Expanded protein expressed increased amounts of several signaling receptors at the membrane and their receptor recycling rate was reduced. This is of interest since merlin is known to interact with a hepatocyte growth factor regulated tyrosine kinase substrate (HRS) (11) that regulates endosome mediated protein trafficking (12) and receptor sorting (32). In addition, Fraenzer et al. (2003) have reported that platelet derived growth factor receptor (PDGFR) is more rapidly degraded in merlin expressing Schwann cells than in cells lacking merlin (10). Recently it has been shown that cells use a specific sorting mechanism of fast and slow maturation of the endocytic vesicles. Certain receptors, such as EGFR, are recycled through a dynamic pool of early endosomes that are highly mobile on microtubules and that mature rapidly towards the late endosomes. This rapid movement and maturation is completely dependent on microtubules; if microtubules are disrupted the dynamic vesicles will non-selectively join all early endosomes and are less efficiently degraded (33). Two papers



have localized merlin to early endosomes (11,13). Thus, it is possible that merlin functions as a linker at the plasma membrane, helping receptor-containing endocytosed vesicles to attach to microtubules. If cells lack merlin, this receptor recycling might be slower, and the receptors would be cleared from the membrane less efficiently. We propose that merlin plays a dual role at the membrane of Schwann cells, partly by transferring early endocytic vesicles to rapidly growing microtubules with the help of Hrs and partly by increasing microtubule polymerization rate thus enhancing the vesicle maturation process.

In the past years several tumor suppressor proteins, including p53, APC, VHL and BRCA1 have been shown to bind and regulate microtubules (15). Here we show that also merlin binds microtubules, regulates their polymerization and has an important role in the establishment of normal Schwann cell morphology. Schwannoma cells from patients display altered morphology with long, multiple extensions (34). According to our study this altered morphology seems to be associated with disturbed microtubule cytoskeleton, linking the interplay of merlin and tubulin to normal Schwann cell development and possibly to schwannoma formation.

## **Materials and methods**

### **Cell lines and antibodies**

U251 glioma cells were maintained in Dulbecco's Minimum Essential Medium (MEM), supplemented with 10 % fetal calf serum (PromoCell, Heidelberg, Germany), 1 % L-glutamine and 50 µg/ml gentamycin (Invitrogen). Cells were fixed in 3,5 % paraformaldehyde, pH 7,5. Primary Schwann cells were isolated and cultured as previously described (35). Anti-merlin polyclonal rabbit antibodies A-19 sc-331, C-18 sc-332 (Santa Cruz Biotechnology, Santa Cruz, CA), 1398 NF2 (36), anti-schwannomin (37), and mouse mAb KF10 (36) were used. TO-PRO 3-iodide probe (Invitrogen, Molecular Probes) was used for DNA staining. Monoclonal anti- $\alpha$ -,  $\beta$ - and -acetylated-tubulin antibodies (Sigma-Aldrich) were used to detect tubulin. Anti-GST polyclonal goat antibody (GE Healthcare) was used to detect GST proteins. Alexa 488-, 568-, 594-

and 633-conjugated goat anti-mouse and goat anti-rabbit antibodies (Invitrogen, Molecular Probes) were used as secondary antibodies in immunofluorescence and HRP-conjugated rabbit anti-mouse and swine anti-rabbit and anti-goat (Santa Cruz) secondary antibodies (DAKO A/S, Glostrup, Denmark) in western blot analysis.

### **Plasmids and protein expression constructs**

The following merlin constructs: isoform I (aa 1-595), isoform II, and isoform I variants S518A, S518D, 1-314, 1-537 and 1-547) in pcDNA3 (Invitrogen) were used for in vitro translation. Luciferase cDNA was used as a negative control. For expression of recombinant GST-merlin fusion proteins, the following constructs were used: merlin N-terminus (aa 1-100 and aa 1-309), merlin  $\alpha$ -helical domain (aa 314-477), C-terminus (aa 492-595) and C-terminus with S518A mutation as described previously (9), merlin 1-537 and merlin 1-547.

Adenovirus construct were made using Stratagene's AdEasy system. Full-length merlin was cloned into the adeno vector and the virus was produced according to manufacturer's instructions in 293 cells. The infection titer was optimized to have 100% efficiency and verified by immunofluorescence staining. EGFP-tubulin construct was obtained from Invitrogen, and transfection to primary Schwann cells was done with Lipofectamine PLUS (Invitrogen).

### ***In vitro* translation and quantification of labeled proteins**

Merlin pcDNA3 plasmids (Invitrogen) were used as a template for a T7-coupled rabbit reticulocyte transcription-translation system (Promega, Madison, WI) in the presence of <sup>35</sup>S-methionine. 5  $\mu$ l of 50  $\mu$ l reaction were run in to SDS-PAGE, gel was dried and exposed to film to determine the size and amount of the labeled protein. For quantification the gel was also exposed to PhosphoImager low energy-plate (GE Healthcare), read by TyphoonImager 9400 (GE Healthcare) and analyzed by ImageQuantTL2003 software (GE Healthcare).

### **GST-fusion protein production**

GST-fusion proteins were expressed in *E. coli* DH5 $\alpha$  and purified following standard protocol. Fusion protein was eluted from the Glutathione Sepharose beads (GE Healthcare) by 5 mM reduced glutathione in 50 mM Tris-HCL pH 8.0, over night at +4°C. Before some tubulin pull-down assays different amounts of N- and C-terminus were incubated in 50 mM Tris-HCl, 150 mM NaCl (pH 8.0) for 30 min at room temperature. The eluted fusion proteins for the PKA assay were dialyzed against 20 mM Tris-HCl, 10 mM MgCl<sub>2</sub>, pH 7.4 at +4°C o/n. Wild type merlin was produced in Sf9 insect cell line. Merlin with an N-terminal GST-tag was cloned into a baculovirus transfer vector pAcG2T (BD Biosciences) and then produced with the BaculoGOLD system (BD Biosciences), Sf9 cells were used to produce recombinant merlin according to user's manual (Invitrogen). Full-length merlin was purified after one day of infection following standard GST-purification protocol, the cells were lysed. The proteins were used immediately after purification.

### ***In vitro* phosphorylation**

GST-proteins were dialyzed against the reaction buffer and run into SDS-PAGE, protein amounts estimated and equal amounts of each construct were used in the *in vitro* phosphorylation assay. Total volume of the reaction was 40  $\mu$ l including PKA reaction buffer (20mM Tris-HCl, 10 mM MgCl<sub>2</sub>, pH 7.4), 200  $\mu$ M ATP and purified human or bovine catalytic subunit of PKA (Sigma-Aldrich). Reaction was incubated 30 min at +30°C and was stopped by adding 20  $\mu$ M PKA inhibitor H89 (Sigma-Aldrich).

### **Tubulin pull-down assay**

Tubulin pull-down was performed with <sup>35</sup>S labeled *in vitro* translated protein, eluted GST-fusion protein or with *in vitro* PKA phosphorylated eluted GST-fusion protein. Equal protein amounts were used in all experiments. 70  $\mu$ g of purified bovine tubulin (Cytoskeleton) was added to tubulin polymerization buffer (80 mM PIPES, 0.5 mM MgCl, 1 mM Ethylene glycol-bis, 1 mM GTP, pH 6.9, 10 % glycerol, 10  $\mu$ M Taxol) to a final volume of 200  $\mu$ l and the microtubules were allowed to polymerize at +37°C for 30 min in the presence of different merlin constructs. After this 50  $\mu$ l were removed and labeled as 'total' fraction and the remaining 150  $\mu$ l were centrifuged at 11 503 g for 30

min at +30°C to collect the polymerized microtubules. Supernatant was removed and the pellet was resuspended in 150 µl of polymerization buffer. Twelve µl of each fraction were analyzed on SDS-PAGE.

### **Western blot**

Primary Schwann cells were lysed in ice cold ELB buffer (150 mM NaCl, 50 mM Hepes pH 7.4, 5 mM EDTA, 0.5% NP40, and Complete protease inhibitor cocktail tablet, Roche) or in mild Triton-X buffer (50 mM Tris pH 7.4, 150 mM NaCl, 1 mM EDTA, 1% Triton-X 100, 1 mM PMSF) including protease inhibitors (Complete), cells were incubated on ice for 15 minutes and centrifuged at full speed in +4 C for 15 minutes. Alternatively, cells were scraped in ice cold PBS, centrifuged briefly and the cell pellet was suspended into Urea-buffer (50 mM Tris, 6 M Urea, pH 7,4). The cells were lysed for 15 minutes and briefly sonicated. The protein amounts were analyzed either by the Bradford assay or by Coomassie staining. Equal amounts of proteins were run into gel transferred into nitrocellulose membrane and blotted with antibodies.

### **Immunofluorescence, laser scanning confocal microscopy and FRAP**

Cells were fixed in 3.5% PFA for 10 min, washed in PBS and permeabilized for 5 min in 0.1% Triton X-100/PBS and blocked at 5% BSA in PBS. Cells were stained with merlin and tubulin antibodies (diluted 1:100 and 1:200, respectively) followed by secondary antibodies or TO-PRO 3-iodide or DAPI nuclear stain. Double stainings were performed sequentially. Coverslips were mounted in DABCO (Sigma) and Mowiol (Calbiochem) or Vectashield (Vector Laboratories, Burlingame, CA) and examined by confocal, Leica SP2 equipped with Ar and Kr lasers (Leica Microsystems, Heerbrugg, Switzerland) or Zeiss LSM 510 META using the sequential scanning mode or by immunofluorescence microscopy (Zeiss Axiophot equipped with AxioCam cooled CCD-camera, Carl Zeiss, Esslingen, Germany).

Live cell imaging was performed in pre-warmed microscope chambers at +37°C with 20 mM Hepes as a buffering agent in the medium. Cells were plated on LabTek borosilicate #1.5 imaging chambers (Nunc, Naperville, IL) and imaged with confocal microscope.

FRAP analysis was performed with Zeiss LSM 510 META confocal microscope, pre-bleach images were obtained after which lasers were turned to full power and region of interest was bleached 50 times, the same settings were used for all FRAP experiments including the region of interest. Data analysis was performed in Zeiss META and in Microsoft Excel.

### **Statistical and image analysis**

All statistical analyses were performed in Excel with Student's T-test using two-tailed distribution and image analysis was performed with Image J 1.36b. Images were processed with Adobe Photoshop.

### ***In vitro* tubulin polymerization and other experiments**

*In vitro* tubulin polymerization was performed on UV-permeable 96-well plates. Tubulin was purified from bovine brain as previously described (38) and recombinant merlin was produced in Sf9 insect cells as described in the GST-fusion protein section. Nocodazole 20  $\mu$ M, Taxol 20  $\mu$ M (Sigma) and MAP's were used as controls in the polymerization reaction. The polymerization buffer (80 mM PIPES, 0.5 mM MgCl<sub>2</sub>, 1 mM Ethylene glycol-bis, 1 mM GTP, pH 6.9, 10 % glycerol, 10  $\mu$ M Taxol) was mixed with tubulin (25  $\mu$ M) and merlin constructs (different amounts) were added on ice. At the beginning of the experiment the 96-well plate was transferred to pre-warmed 96-well plate reader that measured the OD at 350 nm every 5 min at +37°C for 60 minutes. The Nocodazole experiment was performed on primary Schwann cells with or without the re-expression of merlin via adeno-infection. Cells were incubated with 8  $\mu$ M Nocodazole overnight after which the block was released and the cells were fixed at indicated time points. The cells were stained for tubulin and merlin.

### **Acknowledgements**

We would like to thank Niclas Setterblad at the Imaging Department of the Institut Universitaire d'Hématologie IFR105 for valuable help in confocal microscopy and FRAP experiments. The imaging department is supported by grants from the Conseil Regional d'Ile-de-France and the Ministère de la Recherche. In addition we would like to thank all

the personnel in Dr. Giovannini's laboratory for the help with Schwann cell experiments. We are also thankful for H. Ahola for her skillful technical assistance and for L. Heiska for her comments and critical reading of the manuscript. This study was supported by the grants of Department of Defense DAMD17-00-0550 and W81XWH-05-1-0469, Finnish Cancer Organization, Helsinki Graduate School of Biotechnology and Molecular Biology, French embassy in Helsinki, Centre for International Mobility (CIMO), Emil Aaltonen Foundation and Ida Montin Foundation.

## References

1. Gutmann D.H. (1997) Molecular insights into neurofibromatosis 2. *Neurobiol. Dis.*, **3**, 247-261.
2. den Bakker M.A., Riegman P.H., Suurmeijer A.P., Vissers C.J., Sainio M., Carpen O. and Zwarthoff E.C. (2000) Evidence for a cytoskeleton attachment domain at the N-terminus of the NF2 protein. *J. Neurosci. Res.*, **62**, 764-771.
3. Xu H.M. and Gutmann D.H. (1998) Merlin differentially associates with the microtubule and actin cytoskeleton. *J. Neurosci. Res.*, **51**, 403-415.
4. Bretscher A., Chambers D., Nguyen R. and Reczek D. (2000) ERM-merlin and EBP50 protein families in plasma membrane organization and function. *Annu. Rev. Cell Dev. Biol.*, **16**, 113-143.
5. Gonzalez-Agosti C., Wiederhold T., Herndon M.E., Gusella J. and Ramesh V. (1999) Interdomain interaction of merlin isoforms and its influence on intermolecular binding to NHE-RF. *J. Biol. Chem.*, **274**, 34438-34442.
6. Grönholm M., Sainio M., Zhao F., Heiska L., Vaheri A. and Carpen O. (1999) Homotypic and heterotypic interaction of the neurofibromatosis 2 tumor suppressor protein merlin and the ERM protein ezrin. *J. Cell. Sci.*, **112**, 895-904.
7. Nguyen R., Reczek D. and Bretscher A. (2001) Hierarchy of merlin and ezrin N- and C-terminal domain interactions in homo- and heterotypic associations and their relationship to binding of scaffolding proteins EBP50 and E3KARP. *J. Biol. Chem.*, **276**, 7621-7629.
8. Shaw R.J., Paez J.G., Curto M., Yaktine A., Pruitt W.M., Saotome I., O'Bryan J.P., Gupta V., Ratner N. and Der C.J. *et al.* (2001) The Nf2 tumor suppressor, merlin, functions in rac-dependent signaling. *Dev. Cell.*, **1**, 63-72.

9. Alftan K., Heiska L., Grönholm M., Renkema G.H. and Carpen O. (2004) Cyclic AMP-dependent protein kinase phosphorylates merlin at serine 518 independently of P21-activated kinase and promotes merlin-ezrin heterodimerization. *J. Biol. Chem.*, .
10. Fraenzer J.T., Pan H., Minimo L., Jr, Smith G.M., Knauer D. and Hung G. (2003) Overexpression of the NF2 gene inhibits schwannoma cell proliferation through promoting PDGFR degradation. *Int. J. Oncol.*, **23**, 1493-1500.
11. Scoles D.R., Huynh D.P., Chen M.S., Burke S.P., Gutmann D.H. and Pulst S.M. (2000) The neurofibromatosis 2 tumor suppressor protein interacts with hepatocyte growth factor-regulated tyrosine kinase substrate. *Hum. Mol. Genet.*, **9**, 1567-1574.
12. Lloyd T.E., Atkinson R., Wu M.N., Zhou Y., Pennetta G. and Bellen H.J. (2002) Hrs regulates endosome membrane invagination and tyrosine kinase receptor signaling in drosophila. *Cell*, **108**, 261-269.
13. Maitra S., Kulikauskas R.M., Gavilan H. and Fehon R.G. (2006) The tumor suppressors merlin and expanded function cooperatively to modulate receptor endocytosis and signaling. *Curr. Biol.*, **16**, 702-709.
14. Murray J.W. and Wolkoff A.W. (2003) Roles of the cytoskeleton and motor proteins in endocytic sorting. *Adv. Drug Deliv. Rev.*, **55**, 1385-1403.
15. Fisk H.A., Mattison C.P. and Winey M. (2002) Centrosomes and tumour suppressors. *Curr. Opin. Cell Biol.*, **14**, 700-705.
16. Hergovich A., Lisztwan J., Barry R., Ballschmieter P. and Krek W. (2003) Regulation of microtubule stability by the von hippel-lindau tumour suppressor protein pVHL. *Nat. Cell Biol.*, **5**, 64-70.
17. Muranen T., Grönholm M., Renkema G.H. and Carpen O. (2005) Cell cycle-dependent nucleocytoplasmic shuttling of the neurofibromatosis 2 tumour suppressor merlin. *Oncogene*, **24**, 1150-1158.
18. Stokowski R.P. and Cox D.R. (2000) Functional analysis of the neurofibromatosis type 2 protein by means of disease-causing point mutations. *Am. J. Hum. Genet.*, **66**, 873-891.
19. Grönholm M., Muranen T., Toby G.G., Utermark T., Hanemann C.O., Golemis E.A. and Carpen O. (2006) A functional association between merlin and HEI10, a cell cycle regulator. *Oncogene*, in press.
20. Kissil J.L., Johnson K.C., Eckman M.S. and Jacks T. (2002) Merlin phosphorylation by p21-activated kinase 2 and effects of phosphorylation on merlin localization. *J. Biol. Chem.*, **277**, 10394-10399.
21. Morrison H., Sherman L.S., Legg J., Banine F., Isacke C., Haipek C.A., Gutmann D.H., Ponta H. and Herrlich P. (2001) The NF2 tumor suppressor gene product, merlin,

mediates contact inhibition of growth through interactions with CD44. *Genes Dev.*, **15**, 968-980.

22. Xiao G.H., Beeser A., Chernoff J. and Testa J.R. (2002) p21-activated kinase links Rac/Cdc42 signaling to merlin. *J. Biol. Chem.*, **277**, 883-886.

23. Rong R., Surace E.I., Haipek C.A., Gutmann D.H. and Ye K. (2004) Serine 518 phosphorylation modulates merlin intramolecular association and binding to critical effectors important for NF2 growth suppression. *Oncogene*, **23**, 8447-8454.

24. Bretscher A., Edwards K. and Fehon R.G. (2002) ERM proteins and merlin: Integrators at the cell cortex. *Nat. Rev. Mol. Cell Biol.*, **3**, 586-599.

25. Krauss S.W., Lee G., Chasis J.A., Mohandas N. and Heald R. (2004) Two protein 4.1 domains essential for mitotic spindle and aster microtubule dynamics and organization in vitro. *J. Biol. Chem.*, **279**, 27591-27598.

26. Ozer R.S. and Halpain S. (2000) Phosphorylation-dependent localization of microtubule-associated protein MAP2c to the actin cytoskeleton. *Mol. Biol. Cell*, **11**, 3573-3587.

27. Rubino H.M., Dammerman M., Shafit-Zagardo B. and Erlichman J. (1989) Localization and characterization of the binding site for the regulatory subunit of type II cAMP-dependent protein kinase on MAP2. *Neuron*, **3**, 631-638.

28. Grönholm M., Vossebein L., Carlson C.R., Kuja-Panula J., Teesalu T., Alfthan K., Vaheri A., Rauvala H., Herberg F.W. and Tasken K. *et al.* (2003) Merlin links to the cAMP neuronal signaling pathway by anchoring the R1beta subunit of protein kinase A. *J. Biol. Chem.*, **278**, 41167-41172.

29. Lamb N.J., Cavadore J.C., Labbe J.C., Maurer R.A. and Fernandez A. (1991) Inhibition of cAMP-dependent protein kinase plays a key role in the induction of mitosis and nuclear envelope breakdown in mammalian cells. *EMBO J.*, **10**, 1523-1533.

30. Banerjee M., Worth D., Prowse D.M. and Nikolic M. (2002) Pak1 phosphorylation on t212 affects microtubules in cells undergoing mitosis. *Curr. Biol.*, **12**, 1233-1239.

31. Honore S., Pasquier E. and Braguer D. (2005) Understanding microtubule dynamics for improved cancer therapy. *Cell Mol. Life Sci.*, **62**, 3039-3056.

32. Petiot A., Faure J., Stenmark H. and Gruenberg J. (2003) PI3P signaling regulates receptor sorting but not transport in the endosomal pathway. *J. Cell Biol.*, **162**, 971-979.

33. Lakadamyali M., Rust M.J. and Zhuang X. (2006) Ligands for clathrin-mediated endocytosis are differentially sorted into distinct populations of early endosomes. *Cell*, **124**, 997-1009.



34. Rosenbaum C., Kluwe L., Mautner V.F., Friedrich R.E., Muller H.W. and Hanemann C.O. (1998) Isolation and characterization of schwann cells from neurofibromatosis type 2 patients. *Neurobiol. Dis.*, **5**, 55-64.
35. Manent J., Oguievetskaia K., Bayer J., Ratner N. and Giovannini M. (2003) Magnetic cell sorting for enriching schwann cells from adult mouse peripheral nerves. *J. Neurosci. Methods*, **123**, 167-173.
36. den Bakker M.A., Riegman P.H., Hekman R.A., Boersma W., Janssen P.J., van der Kwast T.H. and Zwarthoff E.C. (1995) The product of the NF2 tumour suppressor gene localizes near the plasma membrane and is highly expressed in muscle cells. *Oncogene*, **10**, 757-763.
37. Lutchman M. and Rouleau G.A. (1995) The neurofibromatosis type 2 gene product, schwannomin, suppresses growth of NIH 3T3 cells. *Cancer Res.*, **55**, 2270-2274.
38. Hyman A.A., Drexel D., Kellog D., Salser S., Sawin K., Steffen P., Wordeman L. and Mitchison T.J. (1991) Preparation of modified tubulins. *Meth Enzym.* **196**, 478-486.
39. Utemark, T., Schubert, S.J. and Hanemann, C.O. (2005) Rearrangements of the intermediate filament GFAP in primary human schwannoma cells. *Neurobiol Dis.* **19**, 1-9.

## Legends to figures

### Figure 1.

Merlin colocalizes with microtubules in U251 glioma and primary mouse Schwann cells. **a-i)** U251 glioma cells were synchronized and stained for merlin (green) and tubulin (red). The cells were fixed at different points of the cell cycle, the cell cycle phase was verified by FACS analysis and the localization of the two proteins was analyzed. Merlin and tubulin start to colocalize as cells are approaching mitosis. At this point the two proteins start to accumulate around the nucleus (a). During mitosis merlin localizes to mitotic spindles (b-c, i) and later, during cytokinesis, at the midbody (d-e). After mitosis the two proteins have separate staining patterns when merlin localizes to nucleus and cytoplasm (g). At late G2 tubulin and merlin start to colocalize again (h). **j-m)** In the primary mouse Schwann cells merlin (green) and tubulin (red) colocalize also in the interphase cells (j,l). The colocalization takes place at the membrane areas of the cells and can be seen most clearly when analyzed by confocal microscope and after

colocalization analysis (k,m) (analysis by Image J). Colocalization (white areas) of merlin and tubulin is more easily seen in confluent cultures (k) when compared to subconfluent cultures (m). Nuclei were stained with DAPI (blue). Scale bar 10  $\mu\text{m}$ .

## Figure 2

Merlin binds polymerized tubulin *in vitro*. **A)** A schematic drawing on merlin's domains. **B)** Tubulin binding sites in merlin were mapped by tubulin pull-down assay, in which recombinant GST-merlin was bacterially produced and pulled down with polymerized microtubules by ultracentrifugation. Merlin N (amino acids 1-314), merlin  $\alpha$ -helical (aa 314-492) and merlin C (aa 492-595) constructs were used in the pull-down assay. Total (t), supernatant (s) and pellet (p) fractions with or without tubulin were run into SDS-PAGE, blotted for merlin and analyzed. Merlin N- and C-terminus were recovered from the tubulin pellet. **C)** The binding site was further mapped in merlin by performing a tubulin pull-down reaction with merlin constructs 1-100, 1-537 and the patient mutation 1-547. In the merlin N-terminus binding was mapped to aa 1-100 and in the C-terminus to aa 492-537 (B and C). **D)** *In vitro* translated  $S^{35}$  methionine labeled merlin was produced and used for *in vitro* tubulin pull-down experiments. Merlin was pulled down with polymerized microtubules and the amount of merlin in pellet was analyzed and compared to total amount of merlin (%). Merlin isoforms 1 and 2 both associated with microtubules. Also C-terminally deleted merlin constructs associated with microtubules. A patient mutation construct, merlin 1-547, did not associate with microtubules equally well.

## Figure 3

Intramolecular association and phosphorylation of S518 in merlin inhibits its binding to tubulin. **A)** *In vitro* tubulin pull-down assay was performed with purified GST-merlin constructs. C-terminal merlin (aa 492-595) was incubated with increasing amounts of N-terminal merlin (1-314). Total (t), supernatant (s) and pellet (p) samples were analyzed by Western blot with an antibody recognizing N- or C-terminal merlin. When the C-terminus was saturated with the N-terminus it could no longer bind tubulin. As a control the C-terminus was incubated with plain GST. **B)** C-terminus of GST-merlin was

phosphorylated *in vitro* with PKA and tubulin pull-down assay was performed. When S518 was phosphorylated merlin-tubulin binding decreased markedly ( $p=0.006$ ). The graph shows average  $\pm$  SD of six experiments.

#### **Figure 4**

Merlin enhances tubulin polymerization *in vitro*. **A-B**) Purified tubulin from bovine brain was polymerized *in vitro* at  $+37^{\circ}\text{C}$  and the polymerization was monitored at  $\text{OD}_{350}$ . Full length and 1-547 merlin-GST fusion proteins were produced in Sf9 cells. Taxol was used as a positive control for tubulin polymerization, plain tubulin was used as a zero control and Nocodazole was used as a control for tubulin depolymerization. When full-length merlin (WT) was added into the polymerization reaction, tubulin polymerized more rapidly. Merlin 1-547 was not able to induce tubulin polymerization. With higher merlin amounts polymerization (WTx3) was enhanced. The upper graph **A**) shows all of the controls whereas the lower graph **B**) shows constructs that induced tubulin polymerization with higher magnification. The graph shows an average of three experiments.

#### **Figure 5**

Microtubule cytoskeleton is altered in NF2  $-/-$  Schwann cells. **A-B**) Primary mouse Schwann cells with merlin null background (NF2 $\Delta$ exon2, here marked as  $-/-$ , **B**) and the same cells with adeno-infected wild-type merlin (MWT, **A**) were stained for  $\alpha$ -tubulin and imaged with fluorescence microscope at 20x (left panel) and 40x (right panel) magnification. Microtubule organization is different in merlin  $-/-$  cells and in cells expressing merlin. **C**) Triton X-100 lysates made from the same cells, and from NF2  $+/+$  cells were probed for merlin,  $\alpha$ -,  $\beta$ -, and acetylated-tubulin by Western blot. Ponceau red was used as a loading control. Total lysates of the  $-/-$  and merlin add-back cells were solubilized in 6M Urea buffer and probed for  $\alpha$ -tubulin and merlin.

#### **Figure 6**

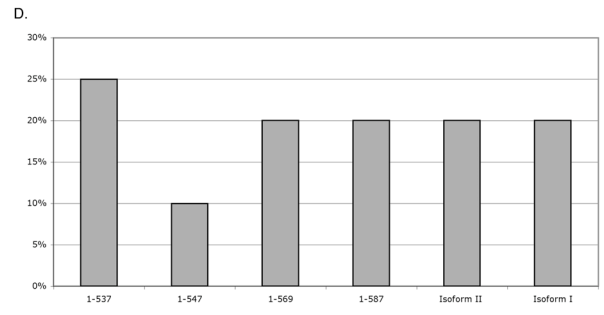
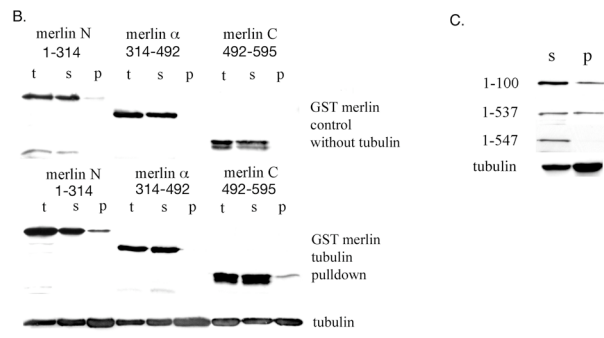
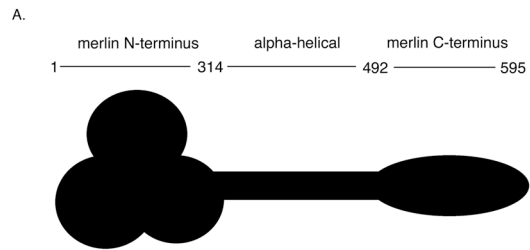
Microtubule recovery is faster in merlin expressing primary Schwann cells. **A**) Primary mouse Schwann cells lacking merlin ( $-/-$ ) or with adeno-infected merlin add-back (MWT)

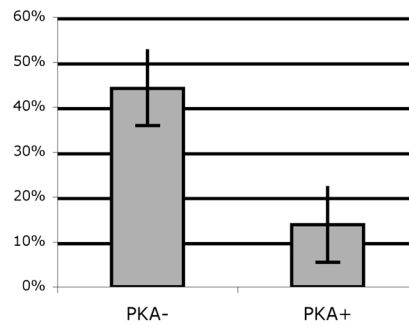
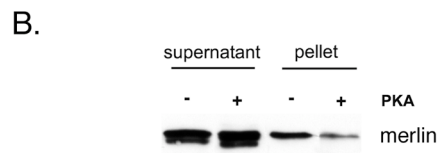
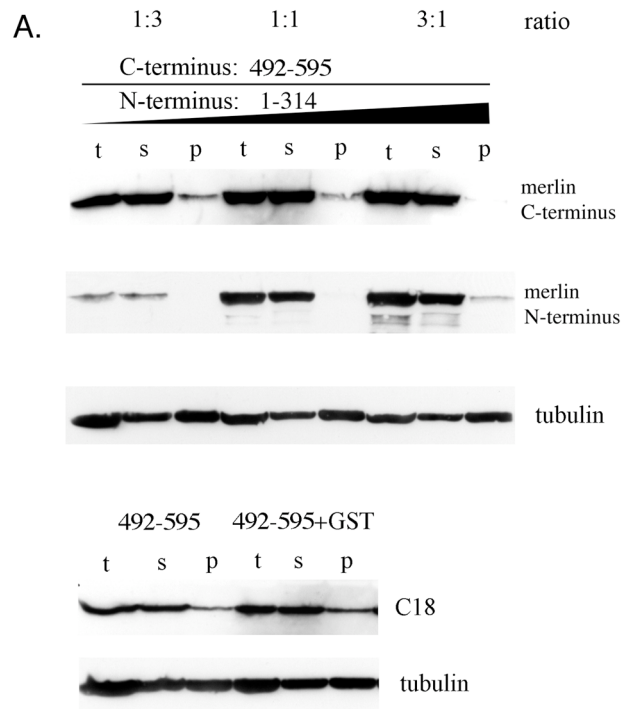
were treated with Nocodazole to depolymerize microtubules. The block was released and cells were fixed at indicated time points. Cells were stained for  $\beta$ -tubulin and imaged with fluorescence microscope at 20x magnification. Merlin induces microtubule formation and enhances Schwann cells in establishing their normal bipolar morphology.

**B)** For FRAP experiments the primary Schwann cells (-/- and MWT) were transfected with EGFP-tubulin and 24 hours after transfection the cells were imaged for FRAP with confocal microscope. Prebleach image was obtained and the region of interest (same region of interest in all the cells) was bleached. Postbleach images were acquired at two-second intervals. From the data the background was subtracted and normalized similarly for all the samples. Eight cells of each construct (-/- and MWT) were imaged and the averaged data was used for data analysis. Cells that were expressing merlin had a faster recovery rate of tubulin than the -/- cells ( $p < 0.001$ ).

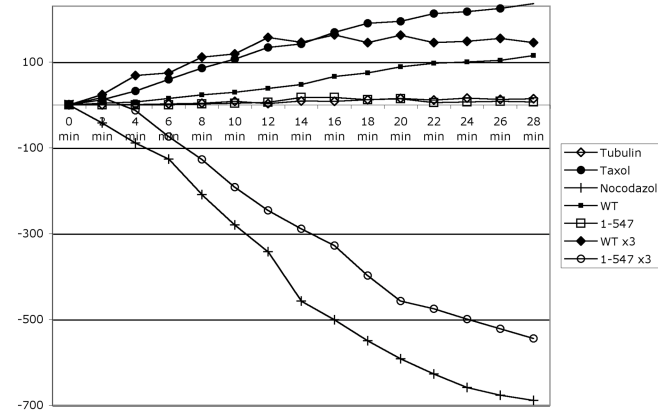
## **Abbreviations**

AKAP	A-kinase anchoring protein
APC	adenomatous polyposis coli
BRCA1	breast cancer gene 1
EGF	epidermal growth factor
EGFP	enhanced green fluorescent protein
EGFR	epidermal growth factor receptor
ERM	e-zrin-radixin-moesin
FERM	4.1-e-zrin-radixin-moesin
FRAP	fluorescence recovery after photobleaching
GFP	green fluorescent protein
GST	glutathione S-transferase
HRS	Hepatocyte growth factor-regulated tyrosine kinase substrate
MAP2	microtubule associated protein
MWT	merlin wild type
NF2	neurofibromatosis 2
PAK	p21-activated kinase
PDGFR	platelet derived growth factor receptor
PKA	cAMP dependent protein kinase A
VHL	von Hippel-Lindau

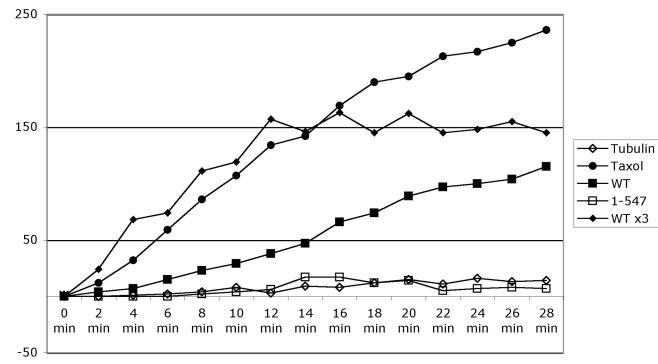




A.

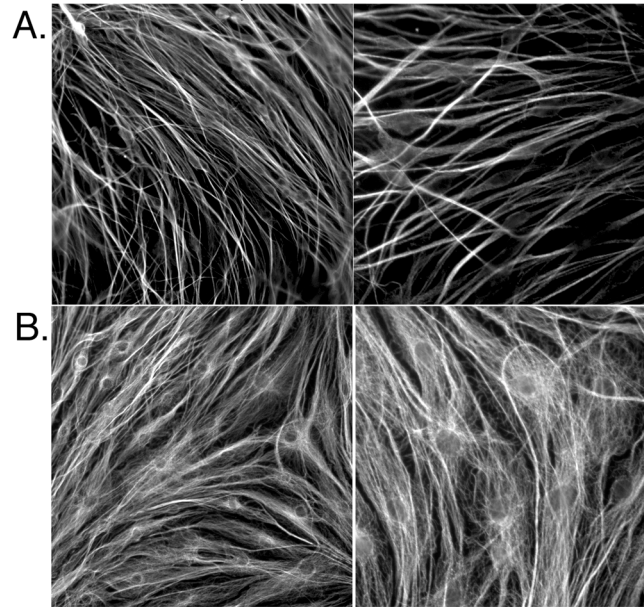


B.





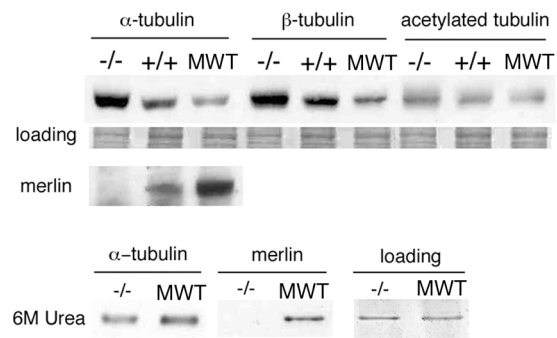
-/- Schwann cells, MWT add-back



-/- Schwann cells

C.

Primary Schwann cells

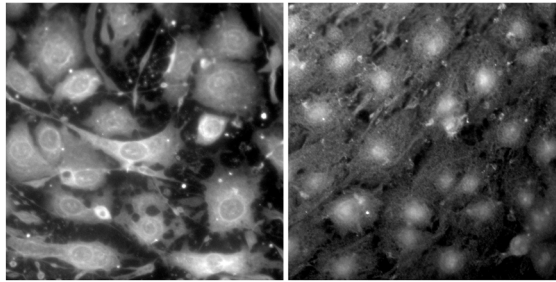


A.

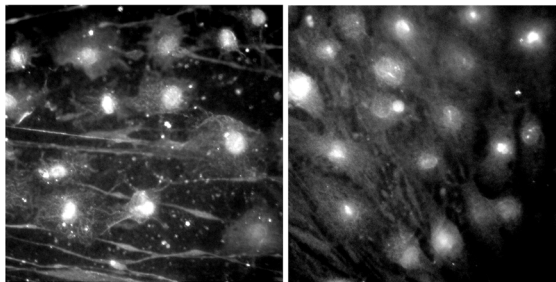
MWT

-/-

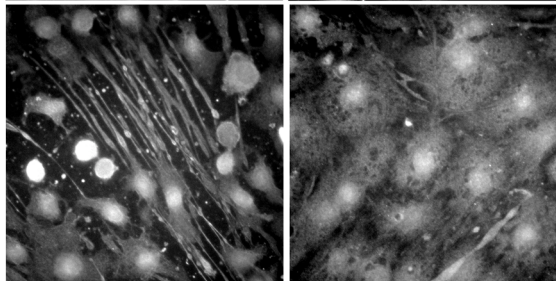
0 min



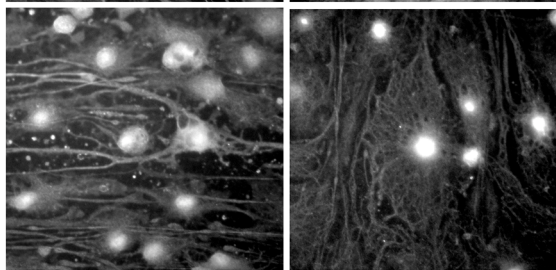
20 min



40 min



150 min



**B.**

**FRAP**

